

AD A0 589 48

ARO 14002.1-EX

LEVEL II

12

DDC FILE COPY

DDC
SEP 20 1978
F

This document has been approved
for public release and sale; its
distribution is unlimited.



THE UNIVERSITY OF MISSISSIPPI
PHYSICAL ACOUSTICS RESEARCH GROUP
DEPARTMENT OF PHYSICS AND ASTRONOMY

AD A058948

DDC FILE COPY

12

Propagation of Sound Through the Atmosphere:
Effects of Ground Cover

H. E. Bass and L. N. Bolen

Technical Report

19 June 1978

U. S. Army Research Office

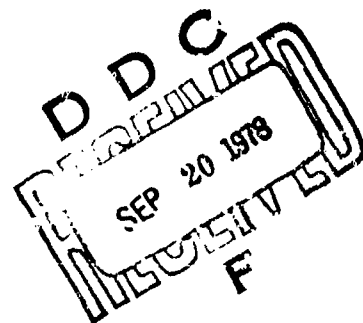
DAAG-29-76-G-0258

Physical Acoustics Research Group

The University of Mississippi

University, MS 38677

Approved for public release;
distribution unlimited.



REPORT DOCUMENTATION PAGE		READ INSTRUCTIONS BEFORE COMPLETING FORM
1. REPORT NUMBER	2. GOVT ACCESSION NO.	3. RECIPIENT'S CATALOG NUMBER
4. TITLE (and Subtitle) 6 Propagation of Sound Through the Atmosphere Effects of Ground Cover.		5. TYPE OF REPORT & PERIOD COVERED Interim June 1976-June 1978
7. AUTHOR(s) 10 H. E. Bass • L. N. Bolen		8. PERFORMING ORG. REPORT NUMBER 14 PARGUM-78-01
9. PERFORMING ORGANIZATION NAME AND ADDRESS Physical Acoustics Research Group The University of Mississippi University, MS 38677		10. PROGRAM ELEMENT, PROJECT, TASK AREA & WORK UNIT NUMBERS 15 DAAG-29-76-G-0258
11. CONTROLLING OFFICE NAME AND ADDRESS U. S. Army Research Office Post Office Box 12211 Research Triangle Park, NC 27709		12. REPORT DATE 11 19 June 1978
14. MONITORING AGENCY NAME & ADDRESS (if different from Controlling Office)		13. NUMBER OF PAGES
		15. SECURITY CLASS. (of this report) Unclassified
		15a. DECLASSIFICATION/DOWNGRADING SCHEDULE NA
16. DISTRIBUTION STATEMENT (of this Report) Approved for public release; distribution unlimited. 12 64 p		
17. DISTRIBUTION STATEMENT (of the abstract entered in Block 20, if different from Report) NA 9 Interim rept. Jun 76-Jun 78		
18. SUPPLEMENTARY NOTES The findings in this report are not to be construed as an official Department of the Army position, unless so designated by other authorized documents.		
19. KEY WORDS (Continue on reverse side if necessary and identify by block number) Sound Propagation; Atmospheric Acoustics; Ground Impedance 18 ARD 1 19 14002.1-EX		
20. ABSTRACT (Continue on reverse side if necessary and identify by block number) Measurements of sound amplitude in the vicinity of a ground plane have been made as a function of frequency of the sound source (100 Hz - 2000 Hz), distance of propagation (5 m - 100 m), and surface conditions. By treating the impedance as an adjustable parameter, the surface impedance as a function of frequency was determined from the measured amplitudes using the theoretical treatment of a spherical wave in the vicinity of a locally reacting surface, developed by Donato (1). Measurements of the amount of energy coupled into		

the ground were also made using geophones below the ground surface.

The impedance measurements were limited to the frequency range 200 Hz to 1000 Hz due to the experimental geometry. In this region, however, the results for three distinctly different surfaces suggest that the impedance can be computed from the specific flow resistance and that grass has little effect on the surface impedance except for decreasing the flow resistance due to the root structure. Experimental studies of surface impedance should include measurements of soil parameters such as density, specific flow resistance, and moisture content so that comparisons can be made between the results from different laboratories and so that a data base for additional theoretical development can be established.

Unclassified

TABLE OF CONTENTS

	Page
1. Introduction	1
2. Experimental Technique	3
2.1 Sound Sources	3
2.2 Amplitude Measurements	4
2.3 Measurement of Seismic/Acoustic Ratio	5
2.4 Measurement of Environmental Conditions	6
2.5 Related Measurements	7
3. Experimental Results	8
3.1 Comparison Measurements	8
3.2 Determination of Acoustic Impedance	17
3.3 Seismic/Acoustic Measurements	20
4. Interpretation of Results	27
5. Summary and Conclusions	44
6. Bibliography	46
Appendix - Computer Program Used to Determine Acoustic Impedance	48

ACCESSION for	
NTIS	Write Section <input checked="" type="checkbox"/>
DOC	Ball Section <input type="checkbox"/>
UNANNOUNCED	<input type="checkbox"/>
DISSEMINATION	
BY	
DISTRIBUTION/AVAILABILITY CODES	
... CIAL	
A	

1.0 INTRODUCTION

Propagation of sound outdoors is influenced by a variety of mechanisms which change the amplitude and phase of the wave. These include:

- Atmospheric Absorption
- Boundary Effects
- Turbulence
- Refraction.

In previous studies, atmospheric absorption was considered in terms of microscopic processes and a technique was developed which allows one to predict atmospheric absorption using simple expressions which are based on the rigorous microscopic treatment (Ref. 2-6). At low frequencies (< 1 kHz), for most conditions, the presence of a boundary will effect the sound amplitude more than atmospheric absorption (Ref. 7). That mechanism is considered in this report. Turbulence can also effect the sound field by destroying coherence and thereby reducing interference which would otherwise occur in the presence of a boundary (Ref. 8). Refraction due to a thermal or velocity gradients also influences the received sound. The measurements reported here were taken under conditions which minimized the effects of turbulence and refraction.

This study of the effect of the ground on outdoor propagation of sound through the atmosphere is the second step in a long range effort to develop procedures to reliably predict sound amplitudes a significant distance from the source and correct measured spectra to free field conditions. The work reported here is the first step in determining the effect of the ground plane.

This report deals primarily with experimental measurements of sound amplitude in the vicinity of a ground surface at ranges out to 100 m at frequencies between 100 Hz and 2000 Hz. These measurements overlap similar measurements made by others and serve to check the experimental procedures as well as extend the data base. Future work will extend these measurements to longer ranges, lower frequencies, and different surfaces. The experimental and theoretical work on the problem of outdoor sound propagation undertaken by this laboratory is meant to complement similar efforts being made by other laboratories most notably the acoustics group at the National Research Council of Canada (Ref. 9,10), and Wyle Laboratories (Ref. 8).

The experimental techniques employed to generate the sound field and measure sound amplitude are described in Section 2. In Section 3, the experimental results are presented. Due to the large number of measurements made, the results are most often reported in terms of acoustic impedance values deduced from a model of the ground surface. Should this model, at some later date, be shown to be inadequate, the raw experimental data can be reconstructed by using the deduced impedance values to calculate the measured sound amplitude. Section 4 provides a tentative interpretation of the experimental results and Section 5 summarizes the results of this study and presents recommendations for future work.

2.0 EXPERIMENTAL TECHNIQUE

The measurements were made by broadcasting sound over a prepared field 300 feet in length. Microphones were placed at intervals down the range at two heights, and recordings were made of the SPL of each microphone. These recordings were then analyzed to determine the surface impedance values of the ground.

2.1 Several speaker systems were constructed for this project. An Altec 515B 15 inch diameter bass driver in a ducted port enclosure was used for the data taken at the Waterways Experiment Station. A combination of 4 of these speakers in an Electrovoice TL 606Q enclosure was used for low frequency measurements (80-200 Hz) in the grass field in Oxford. High frequency data were taken with a horn system composed of 4 University ID-60 compression drivers loaded by an inverted cone truncated with a 4 inch diameter opening.

The data analysis program assumes a spherically diverging wave front. Although a theoretical treatment for a non-spherical wave is possible, the spherical geometry eases physical interpretation of the results. The requirement for a spherical wave front dictates that the source of sound be approximated as a point source. At frequencies below 100 Hz, this represents no problem; the speakers used can be considered a source of spherical waves. Each speaker system utilized was tested to determine its directivity pattern as a function of frequency. An increased directionality at higher frequencies is characteristic of radiating circular pistons. As a result of these measurements, data above 200 Hz was not taken using the large, low frequency driver systems. The high frequency system was capable of producing a uniform distribution of sound with a deviation from sphericity of ± 2 dB to a frequency

of 200 Hz.

2.2 Measurements were made of the amplitude of the sound by microphones placed 1 and 2 meters above the surface of the ground at 50 foot intervals from 50 to 300 feet from the speaker (acoustic to seismic measurements were made as close as 5 m from the source). A single stationary reference microphone was placed at ground level 50 feet from the speaker to measure any variations in sound intensity from the speaker system during the course of the experiments.

Two types of signals were broadcast over the range. Octave bands of pink noise of one minute duration were used in the original experiment at WES. Later data taken at the farm in Oxford used bands of pink noise 1/2 octave in width centered about each 1/3 octave center frequency from 80 to 2000 Hz. Data were also taken in this field using sweep test tones from 80-200 Hz and 180-2000 Hz. In each case the appropriate speaker system was used to assure the sphericity of the transmitted wave.

The speaker system was suspended on a large crane at WES and speaker heights varied from 1 to 10 meters above the ground. In Oxford, the speaker system was suspended from a cross member on a telephone pole, and most of the data were taken with a speaker height of 10 feet.

The microphones used for the amplitude measurements were B&K 4125 1/2" Condenser Microphones with a B&K 2642 preamplifier and B&K 3810 power supply. A GR 1962-9602 Electret microphone was used to monitor the speaker level. The signals from the microphones were recorded on a pair of Uher 4200 2 track tape recorders in a special environmental package. These data were then played back into a GR 1554-A 1/3 octave band analyzer for the analysis of pink noise or into a HP 3580A analyzer synchronized for use as a tracking filter

for the sweep test tones.

The system was calibrated by recording the output from a GR 1562 sound level calibrator on each microphone - recorder channel at the beginning and end of each run. No measureable gain shift was observed during the course of any run.

2.3 Measurements of the ratio of the seismic and acoustic energy were conducted in two series of experiments at the Waterways Experiment Station in Vicksburg, MS. Seismic data were obtained using scientific triaxial geophones which are capable of detecting microseismic signals in the vertical, radial, and horizontal directions with a frequency range from 1 Hz to 600 Hz. During field calibration, the amplifiers for the geophone signature channels were set to the gains to be used during each test. A sine wave voltage was applied to the amplifier and adjusted to give a specific calibration voltage. The signal amplitude from the geophone was then related to the seismic velocity in cm/sec using the calibration sensitivity furnished with each geophone.

The acoustic transducers consisted of the 4 B&K 4125 capacitor microphones placed at the surface of the ground on foam mounts. The microphones were calibrated using the GR 1562 calibrator.

The amplifiers used were commercial units with gains of 10 to 2500 and a flat frequency response from DC to 10,000 Hz. The recording system consisted of a 14 channel magnetic FM tape recorder operating at 7 1/2 inches/sec with a flat frequency response from DC to 2500 Hz.

The data collected consisted of signal levels from microphone and vertical geophone pairs located on a vertical line at distances of 10, 30 and 60 meters from the sound source. Three sources of noise were used; a frequency

sweep (80-2000 Hz), octave band noise (45-2000 Hz) and an impulse (broad band noise from a .45 caliber line thrower). The ratio of the acoustic to seismic energy was measured at each distance for various speaker heights in order to investigate the coupling of acoustic energy to seismic energy as a function of the angle of incidence of the sound.

Data from these measurements were transposed at WES from FM to 2 channel direct record signals and sent to our laboratory for analysis. A Crown DC 500 tape recorder was used to play back the signals which were analyzed using 1/3 octave and correlation analyzers.

2.4 Differences in air temperature with height above the earth may have a strong effect on the propagation of acoustic waves due to refractive effects. Measurements of air temperature versus height were made at each site during the course of each test period. The temperature and wind velocity was monitored using a Wallace GGA23S Thermo-Anemometer with a N1125ANE probe. A log was kept of these variables during each testing period. Temperature gradients of less than 3°F for a 10 meter height increase were always required for data acquisition and in general, the gradients were less than 2°F for 10 meters. Data was not collected when the wind speed exceeded 3m/sec.

The seismic measurements also required a low background noise level. The major source of seismic noise at WES was a road approximately 400 meters from the test site. Most of the data were recorded in the late afternoon and evening when the amount of traffic was small.

An estimate of the effect of air turbulence on the acoustic signal was obtained by measuring the coherence length of the propagating sound waves. Since a single source was producing the direct and reflected wave, interference effects from phase cancellation could be observed only if the

waves were coherent over the path length involved. White noise and bands of pink noise were broadcast over the range. The acoustic signals received by microphones 30 meters apart were analyzed on a Honeywell SAI43A Correlation Analyzer. The coherence length measured in these experiments was greater than 30 meters for the noise. The coherence length is frequency dependent and it will be noted in the results that above 1 kHz, turbulence led to a loss of coherence at the greater propagation distances.

2.5 The soil at each site was measured and classified. At the WES site, the soil is a brown to dark brown heavy silt loam. The texture of the subsoil ranges from heavy loam to silty clay loam. The site at Oxford was sampled by the local USDA Sedimentation Laboratory and a series of physical classification tests were run. The site was located in a valley bottom covered with very recent alluvium deposited over Kosciusko and Tallahatta foundations. The soils are paleudalts and are predominately a silt loam with greater than 50% silt and greater than 7% clays. In the region of 200-350 feet on the test range the soil contains more loamy sand.

Moisture content of the soil can greatly affect its flow resistance and acoustic properties. The soil was sampled at the time of each measurement and the water content is included as a parameter in each of the measurements reported.

3.0 EXPERIMENTAL RESULTS

The experimental data is numbered according to the sequence in which it was collected. Table I gives a brief synopsis of the various data collection runs. A total of sixteen sets of data were collected (excluding seismic data) each consisting of SPL measurements at four to eight microphone locations, two to six microphone heights, and typically 13 different frequencies. All data was collected at least twice for averaging. This amounts to 12,000 data points. There is no way to present all this data in a report of acceptable length. Instead only that data needed to illustrate specific points will be presented. Further, this data will be discussed in the order appropriate to a logical development of the topic, not in the order in which they were collected.

3.1 Comparison Measurements.

The ground cover most thoroughly studied in terms of a boundary to acoustic propagation is "institutional grass". This is the type cover usually encountered on college campus lawns, around government buildings, etc. Although the actual grass type varies, it is almost always well trimmed, uniform, and relatively dense. The earth under the grass has usually gone many growing seasons without tilling.

Measurements of sound amplitude over institutional grass on the UM campus are presented in Figures 1-2. All levels are referenced to the 50 ft. position. These data (Runs 11 and 12) were collected with the speaker system 5.3 ft. from the ground plane and two microphones (one meter and two meters above the ground) which were moved between data collection locations 50 ft., 75 ft., 100 ft., 150 ft., and 200 ft. from the speaker. The source was driven

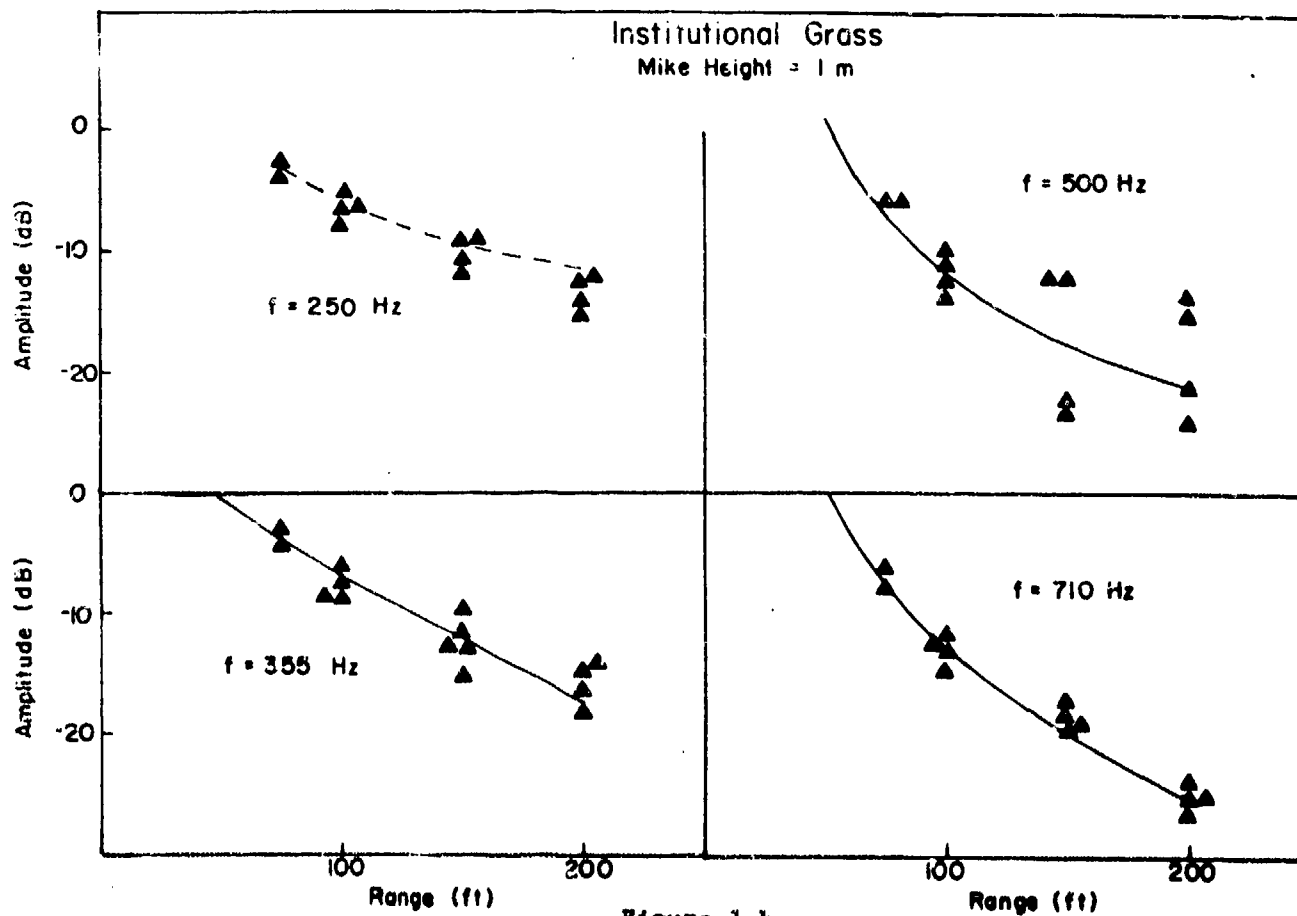
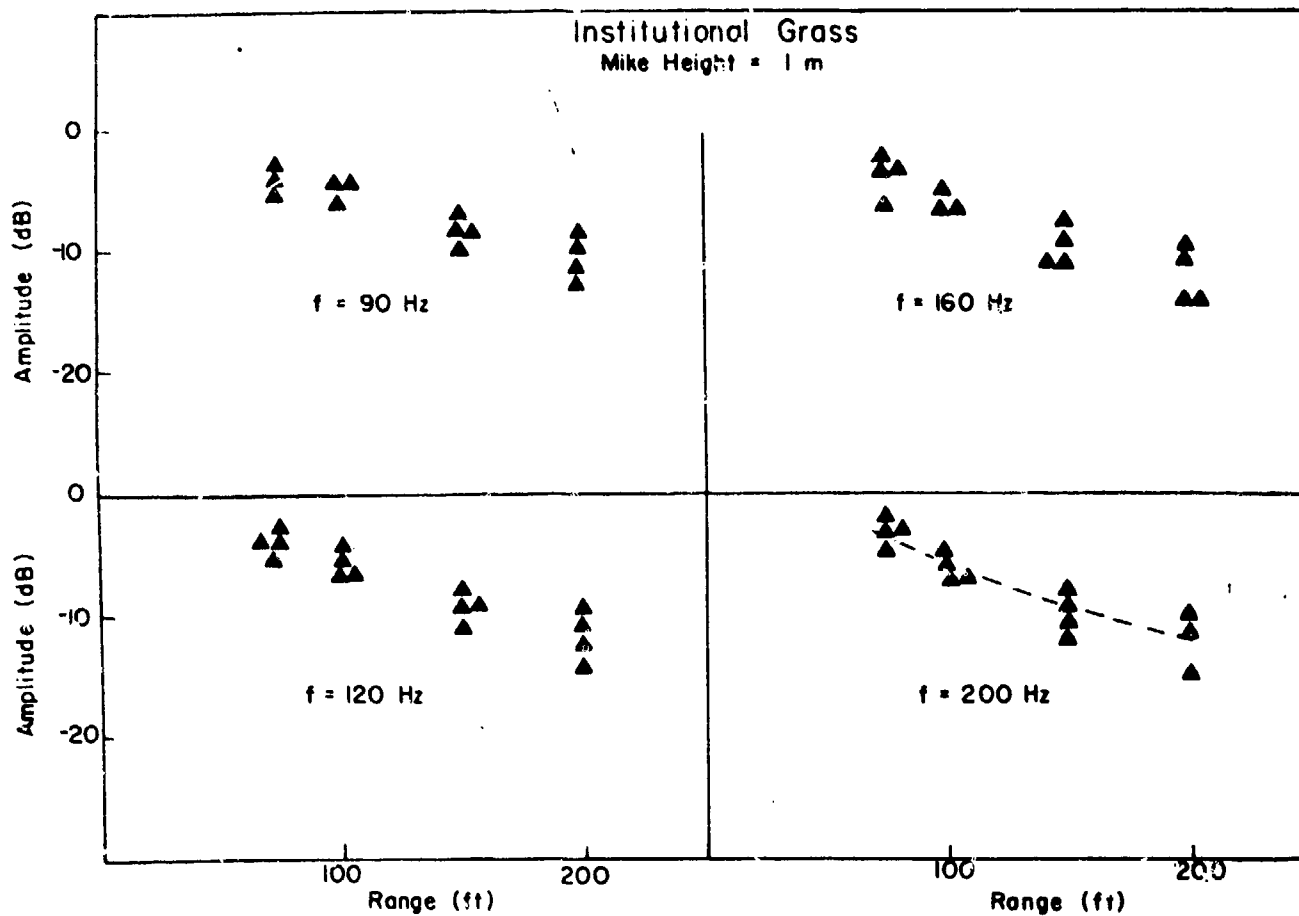
Table I

Experimental Conditions

Run No.	Location	Type of Surface	Moisture Content	Type of Source	Date	Comments
WES I	Waterways Exp. Station	Scattered grass		Bands of noise		Ground frozer
WES II	Waterways Exp. Station	Scattered grass		Bands of noise		
2	Sorghum Sudan	Bare surface - seeds in the ground		Octave band pink	5-26-77	
3	Sorghum Sudan	Grass barely visible		1/2 Octave band pink	5-31-77	
4	Sorghum Sudan	Sparse growth		1/2 Octave band pink	6-8-77	
5	Sorghum Sudan	Sparse growth		1/2 Octave band pink	6-9-77	
6	Sorghum Sudan	10"-12" high grass			6-24-77	
7	Sorghum Sudan	22" grass	48% by weight	1/2 Octave band pink	7-8-77	
8	Sorghum Sudan	22" grass - bulk density of ground 1.27 kgm/cm ³	10% by weight		7-12-77	
9	Sorghum Sudan	25" grass - grass density 8.6 mg/cm ³	8.6% by weight	1/2 Octave band pink and sweep tones	7-22-77	

* Run 1 aborted

10	Sorghum Sudan	1.1m grass	-	1/2 Octave band pink and sweep tones	8-2-77
11	Band field	1 1/2" Institutional Grass	-	Sweep tones 250 Hz-2KHz	8-5-77
12	Band field	1 1/2" Institutional Grass		Sweep tones 90 Hz-200 Hz	8-10-77
13	Sardis Reservoir Beach	Sand	5.6% by weight	Sweep tones	8-16-77
14	Sorghum Sudan	Field cut	-	Sweep tones	9-5-77
15	Sorghum Sudan	Field cut	22%	Sweep tones	9-20-77



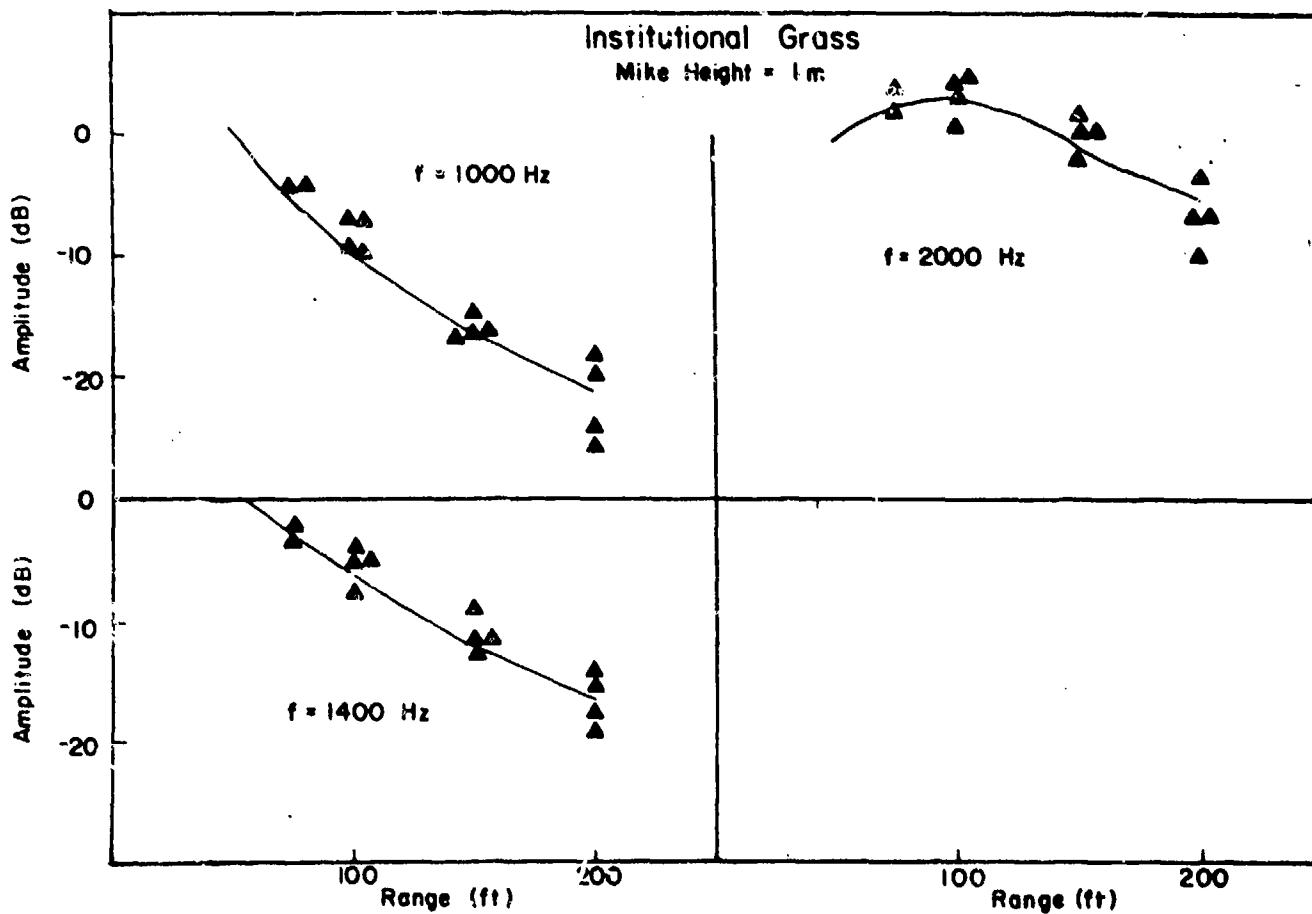


Figure 1 c

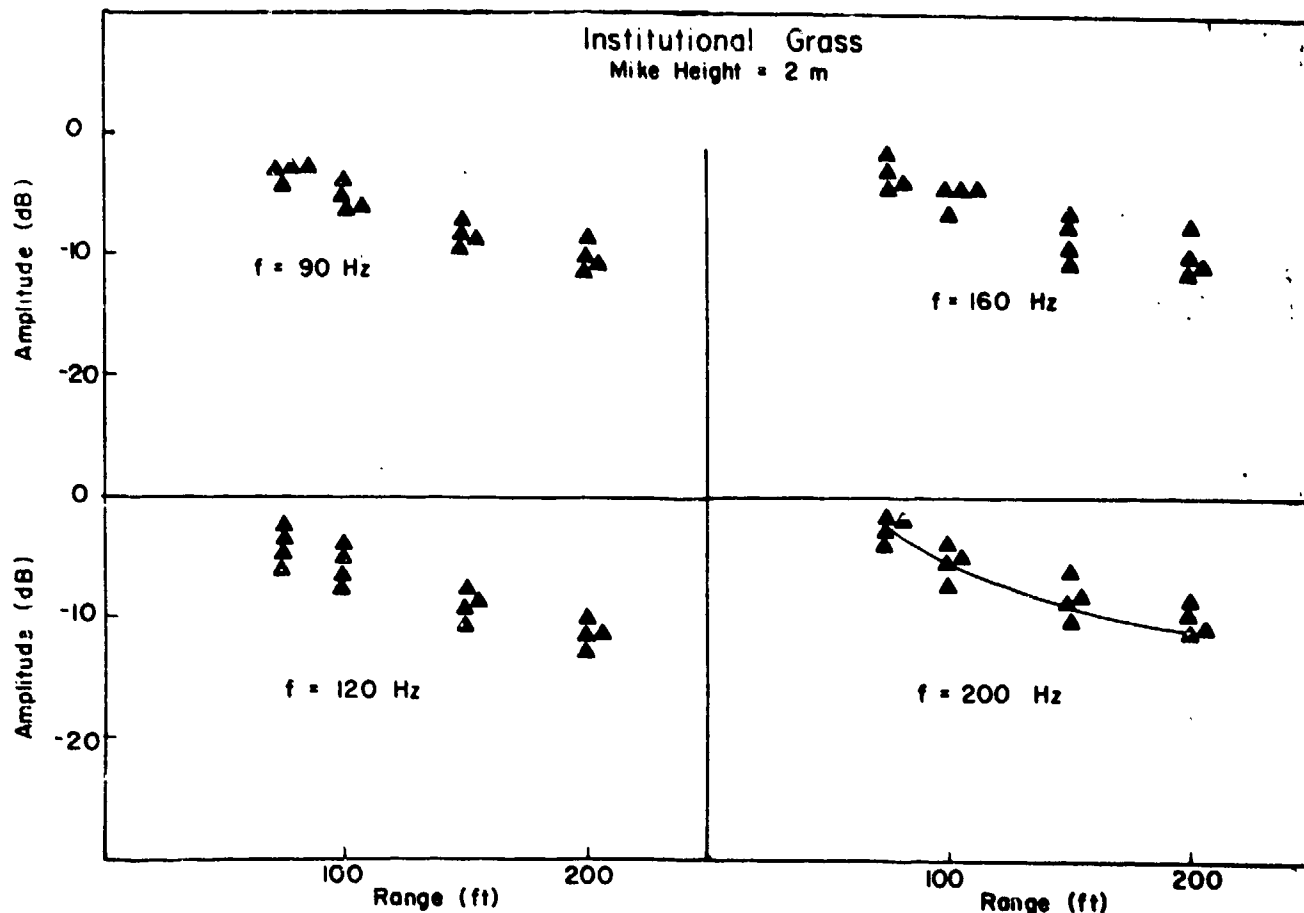


Figure 2 a

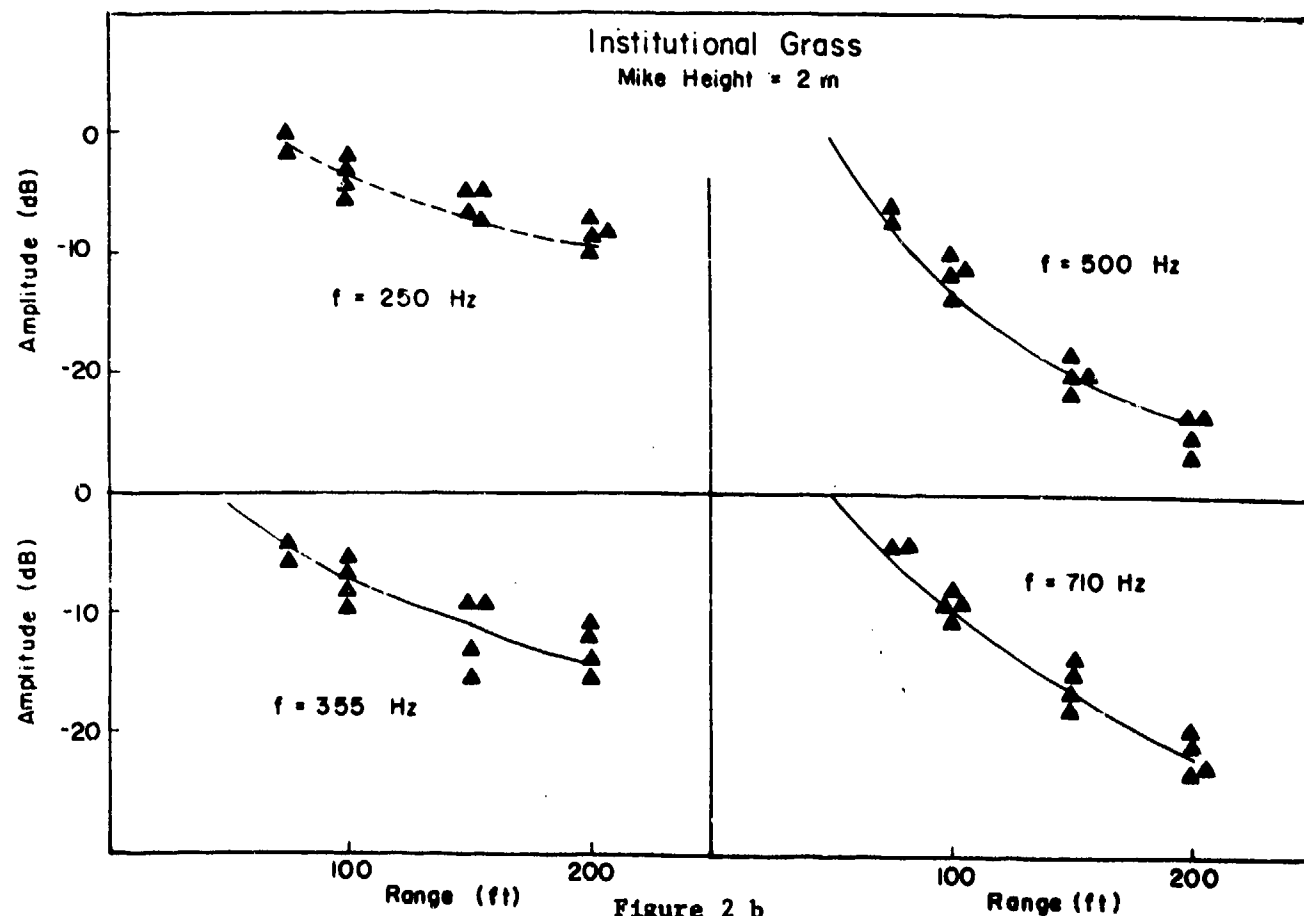


Figure 2 b

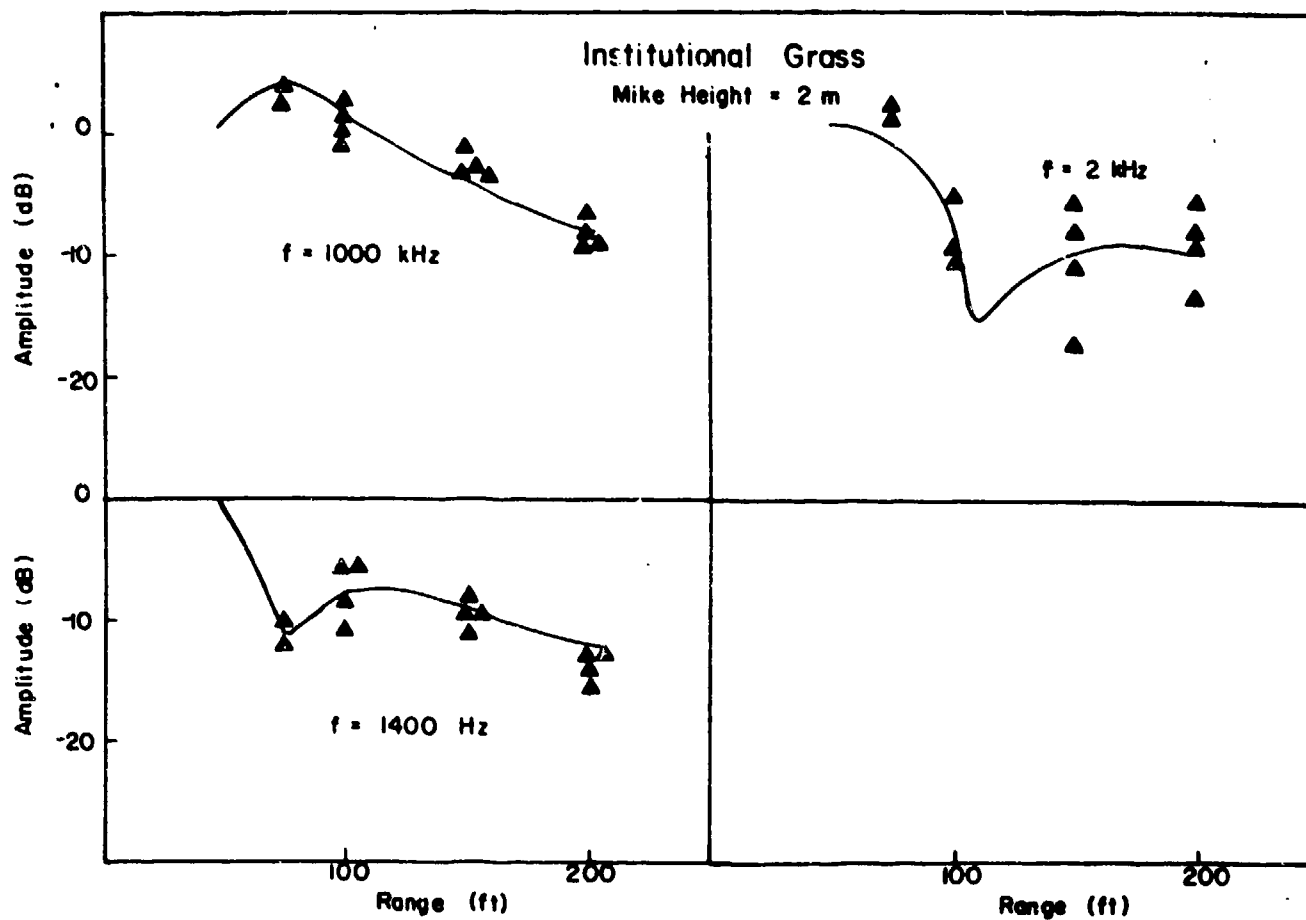


Figure 2 c

by a prerecorded sweep tone extending from 200 Hz to 2 kHz (Run 11) and 45 Hz to 200 Hz (Run 12).

Referring to Figures 1-2, it can be seen that the data at low frequencies are reproducible to within about 2 dB. This 2 dB variation can probably be attributed to variations in speaker output, noise, and instabilities in the recording system. A variation of ± 1 dB was anticipated and is considered acceptable. At the larger ranges, the fluctuations exceed 2 dB. This is a result of decreased signal to noise ratio but since this type of scatter should be random, by taking four points, the true SPL should be determined ± 1 dB. As the frequency increases, so does the scatter in data. At 500 Hz, this situation is worst. The first interference minimum occurs near 500 Hz. At the interference minimum, the acoustic signal decreases by as much as 30 dB thereby decreasing the S/N ratio by a like amount. Also, since interference relies on coherence between the direct and reflected waves, when the reflection coefficient is high (as it was for the field used) a small loss of coherence due to a transient turbule will greatly affect the recorded SPL. This combination of factors reaches a maximum near the first interference minimum in most all cases. Since the effect of turbulence and noise is to increase the S , the lowest value of SPL should be taken as the correct value unless it is much different from the general trend of the data. In practice, the lowest values were weighted by a factor of two relative to intermediate values (weighting of 1) when comparing to theoretical curves.

Referring again to Figures 1 and 2, the solid lines were computed from the theory of Donato¹ using the impedance as an adjustable parameter to achieve the best fit between theory and experiment. It can be seen that the theory is in excellent agreement with measurement. As will be discussed later,

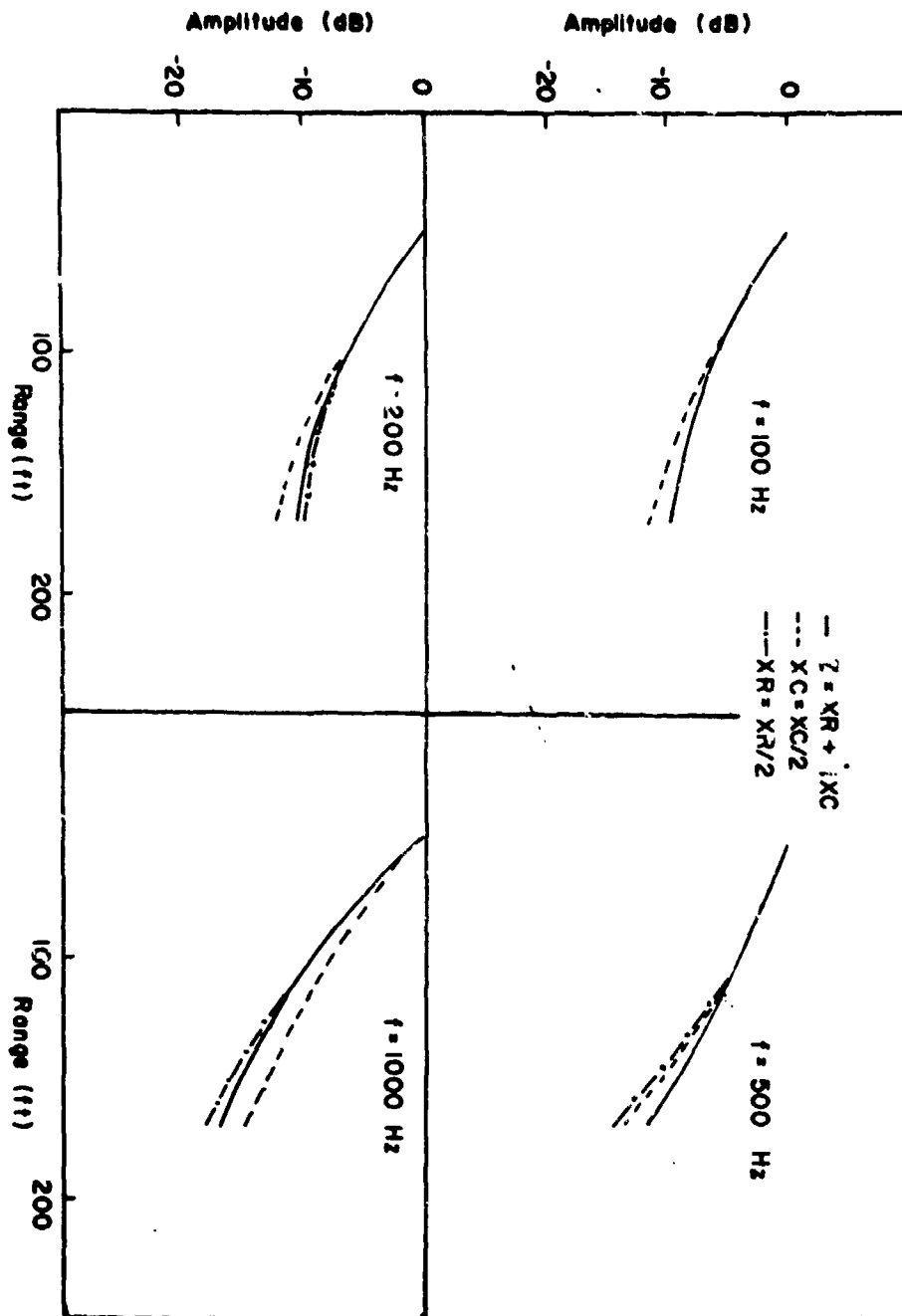


Figure 3

these curves are relatively independent of values chosen for the impedance at frequencies below 200 Hz. Considering the excellent agreement demonstrated here, it appears that the only quantities necessary to represent the experimental data are values of impedance. By selecting values of impedance which provide amplitude versus distance curves in good agreement with experiment, the large quantity of data can be represented by a few graphs of impedance versus frequency.

Before presenting the data in terms of impedance values, one problem should be noted. Figure 3 shows theoretical amplitude versus range curves for four frequencies with reasonable estimates of impedance ($Z = X_r + iX_c$). Also given there are curves computed when X_r and X_c are halved. For the lower frequencies, the computed amplitude curves are very insensitive to values of X_r and X_c becoming more sensitive at higher frequency. This means that impedance values determined from amplitude versus distance curves are going to be uncertain to at least a factor of two with the uncertainty increasing at lower frequencies. At the same time, however, predicted amplitudes are less sensitive to impedance at lower frequencies hence even a very uncertain value of Z enables one to compute the amplitude accurately. Also note that at 500 Hz, a variation in X_r gives the same result as a variation in X_c . So if impedance values are to be determined by fitting the data, either X_r or X_c could be varied.

3.2 Determination of Acoustic Impedance.

In order to represent our data in terms of impedances, an iterative search procedure was used. First, reasonable guesses were made for X_r and X_c and at a particular frequency the amplitude was computed for each experimental range and microphone position. The difference between measured and computed amplitudes was computed and stored as the error. Next, X_r and X_c were each

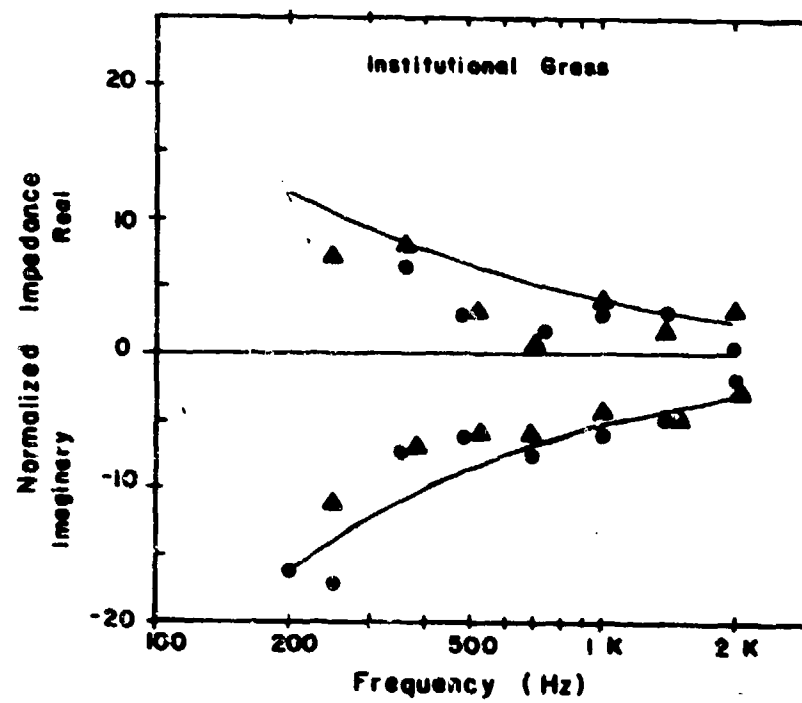


Figure 4

incremented a predetermined amount plus and minus creating an array of X_r 's, and X_c 's for which new errors were computed. The value of X_r and X_c giving the least error was used as a new starting point for the next cycle in the iterative procedure with a smaller increment. This process was continued until the best X_r and X_c were determined to within $.1 \rho_0$. A copy of the computer program is attached as Appendix 1. Results of this iterative process are presented in Figure 4 along with curves of impedance values by Piercy, et.al. The agreement between Piercy's data⁹ and ours is very good considering "institutional grass" in Canada might differ from "institutional grass" in Mississippi. Impedance values were not determined below 200 Hz due to the large range of Z 's which would provide good agreement with measurements. The solid circles were computed by simultaneously fitting data for two microphone heights. The triangles were determined by fitting data at each microphone height separately and then averaging the results.

From the study of sound propagation over "institutional grass" we determined that:

1. The experimental procedure gave reproducible results within ± 2 dB.
2. The theoretical treatment of Donato is in excellent agreement with measurements when appropriate values of impedance are selected (it should be noted that the most controversial aspect of Donato's theory, the magnitude of the surface wave, was not a factor in these measurements).
3. The impedance values determined from amplitude measurements are subject to an error of \pm a factor of two increasing at frequencies below 200 Hz.
4. Impedance values determined in the manner described here are in excellent agreement with measurements at other laboratories for "institutional

grass".

These results indicate that the measurements over different types of surfaces described in the following should give reliable values of impedance.

3.3 Seismic/Acoustic Measurements.

The sound field above the surface was measured with a microphone giving a value of $|p|$; the seismic velocity below the surface was measured with a geophone giving a value of $|v|$. The ratio of $|v|$ to $|p|$ was referred to as the seismic/acoustic or acoustic to seismic coupling ratio (or coupling coefficient), η , given in units of cm/sec/ μ bar. It should be noted that η is closely related to the impedance $Z (= p/v)$.

Typical results for η as a function of frequency measured on the UM campus are given as Figures 5 thru 7. The results of the WES measurements are given in Reference 11; they are in general agreement with the UM measurements. Motion was measured in three directions; vertical or perpendicular to the surface; radial, parallel to the surface along the source - geophone line and; transverse or horizontal, parallel to the surface and perpendicular to the source - geophone line. Referring to Figure 5, it can be seen that the coupling ratio decreases with frequency for all three at about the same rate and each shows a maximum near 100 Hz. A maximum near 90 Hz was observed for the WES measurements.

Impulsive measurements at WES (Figure 8) indicate that the seismic signal arrives at the same time as the acoustic signal. This was interpreted to indicate that the energy to which the geophone was responding was coupled in close to the geophone position with little or no contribution from other points on the surface between the source and geophone. In this case, the angle of incidence is well defined even for a spherical source. Figure 6 shows the

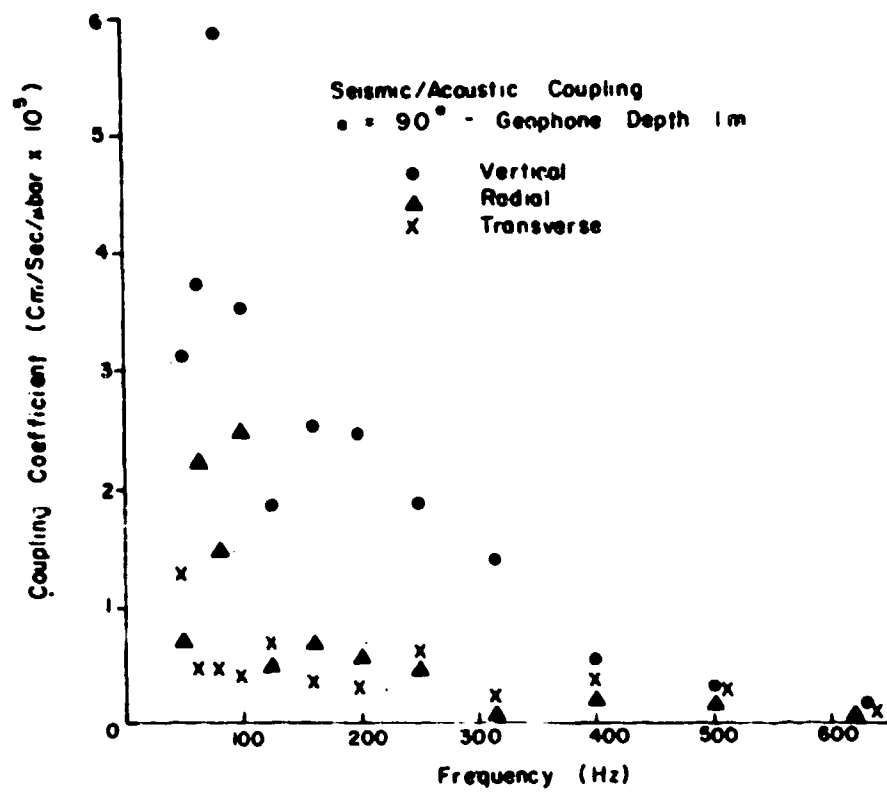


Figure 5

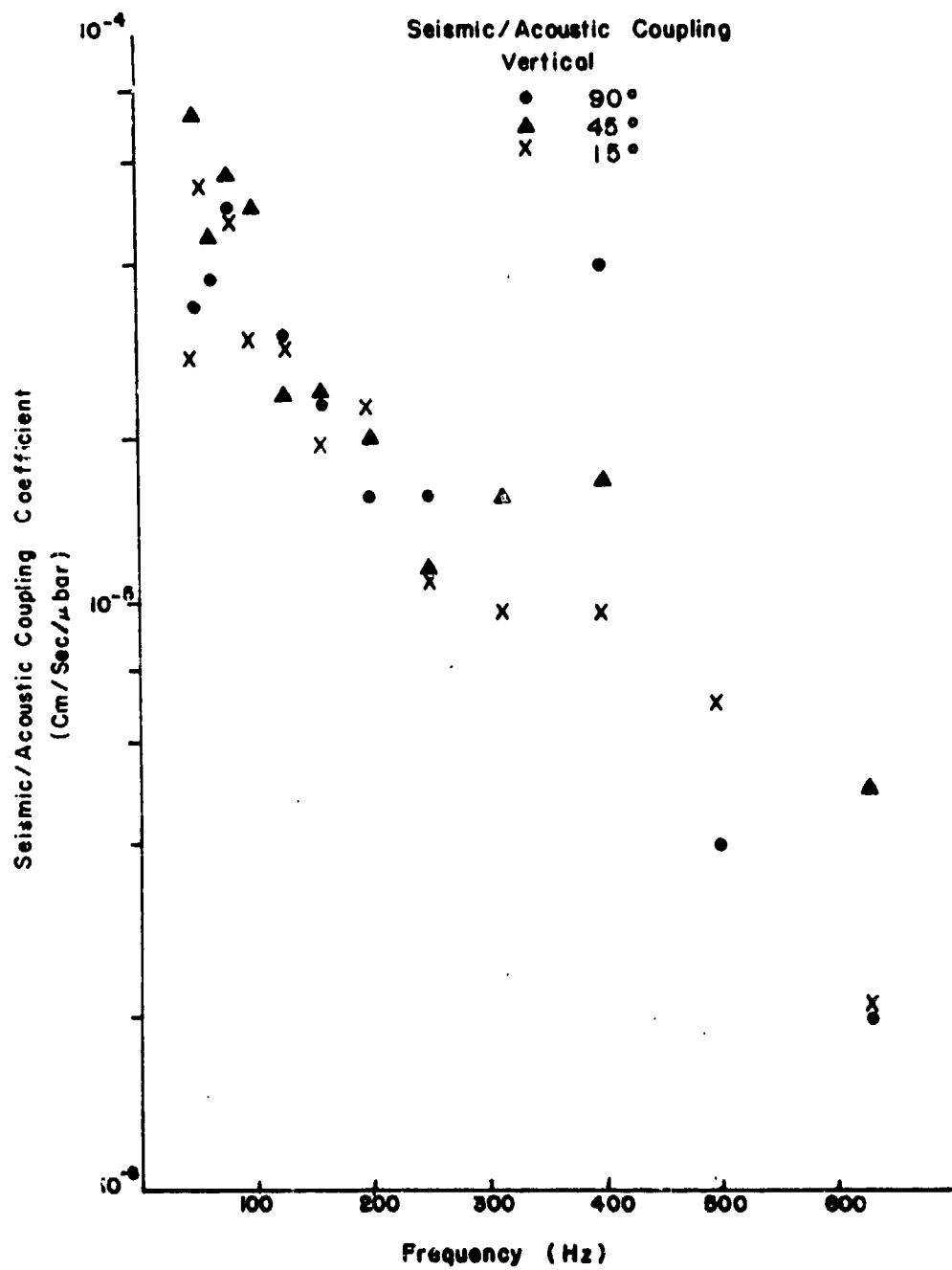


Figure 6

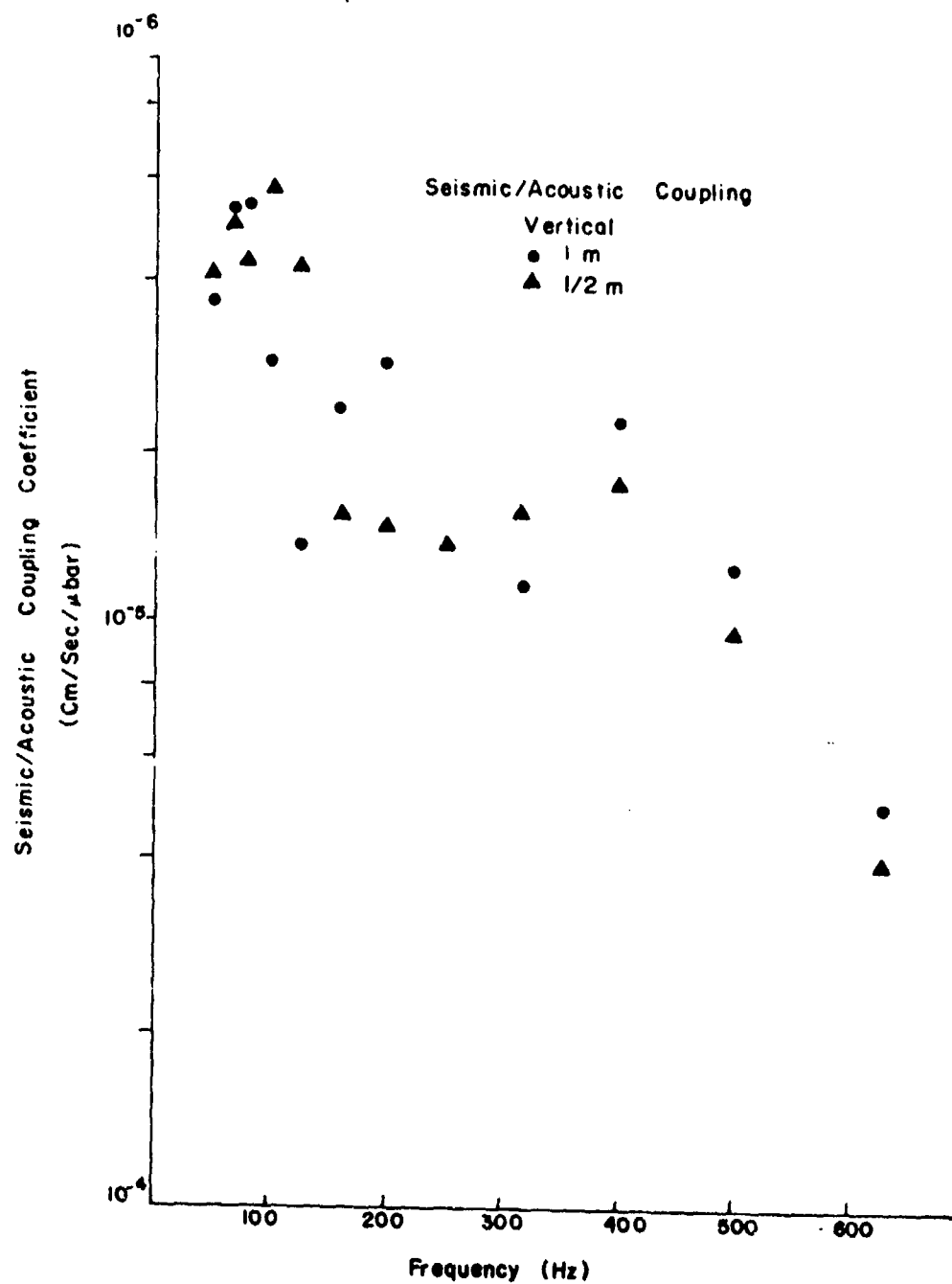


Figure 7

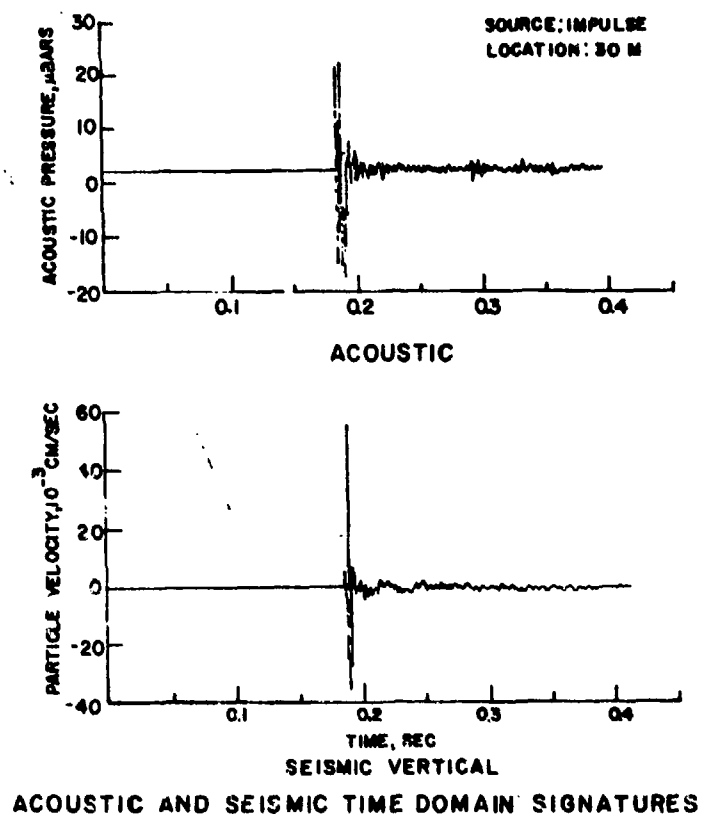


Figure 8

dependence of η on the angle of incidence of the incoming sound. And Figure 7 shows the dependence of η on depth of the geophone. It can be seen that the coupling ratio, η , is not very sensitive to angle of incidence; there is no clearly identifiable trend.

These two results, the frequency and angular dependence of the coupling ratio, are in sharp contrast to predictions assuming the ground is a homogeneous elastic medium (Ref. 11) which predicts a strong angular dependence and little or no frequency dependence of η . The magnitude of η is measured to be much larger than the predicted value near 100 Hz (by a factor of 5-8); the frequency dependence measured is much stronger than predicted; and the angle of incidence dependence measured is much less than predicted.

The values of the ground properties necessary for the elastic theory were measured independently at WES. The density was 2 gm/cm^3 , the compressional velocity was 340 m/sec, and the shear velocity was 155 m/sec. These values were used to compute the theoretical curves for comparison to UM data. Although the two soils were somewhat different, an independent measure of density and Rayleigh wave velocity at UM gave values close to the WES site hence we felt justified in using the WES values in the calculations; small differences in these parameters do not affect frequency or angular dependence significantly.

The inadequacy of elastic theory in predicting the seismic response, though quite intriguing, is not of primary interest here. The sound field above the surface is accurately predicted if the surface impedance is known so for now only those aspects of the seismic/acoustic ratio which provide some insight into the nature of the interaction which effects Σ will be considered. These results can be summarized as follows:

1. At high frequencies η decreases implying that less energy is being coupled into the earth or that the energy is being absorbed by the upper

layer. The surface impedance decreases with frequency indicating that less energy is being reflected hence the energy must be absorbed.

2. At low frequencies, η increases (ignoring the possibility of a peak near 100 Hz) and so does Z .

Based on these results, one might argue that at low frequencies, the sound entering the porous surface is coupled into the earth and $Z \rightarrow Z_{\text{earth}}$ with the porous material acting as an impedance matching layer thus increasing η . If this is the case, at low frequencies (less than 100 Hz) Z should approach ρc of the earth and η should approach elastic predictions. At higher frequencies the energy entering the surface is dissipated by the upper fibrous structure and is now coupled into the earth.

4.0 INTERPRETATION OF RESULTS

In order to discuss the results, it is necessary to first put the outstanding problems involved in predicting the sound pressure in the vicinity of a ground plane in perspective. If the ground plane is assumed to be a locally reacting porous medium, we and others have found that present theoretical treatments which assume a point source give reasonable agreement with experiment when the impedance is used as an adjustable parameter. The acoustic theory of Donato¹ was used to analyze the results of this work giving impedance values reported in the previous section which are generally consistent with impedance values reported by others when the same locally reacting model was used. The results reported here extend to a maximum range of 600 ft. and a lower frequency limit of 100 Hz. In this range, the surface wave predicted by the theory used to analyze the data was not calculated to be a significant fraction of the measured amplitude. We can only say for sure, then, that in the frequency range studied, the locally reacting surface model as applied by Donato agrees with experiment when the impedance is treated as an adjustable parameter.

The use of the term impedance can, in itself, lead to confusion. The most common definition for impedance is

$$Z = \frac{P}{u} = X_r + i X_c \quad (1)$$

where P is the instantaneous pressure and u is the instantaneous velocity. Since acoustic pressure is continuous across a boundary (within a solid the pressure is the diagonal element of the stress tensor, σ_{xx}), the impedance of the soil is measured directly in a seismic/acoustic measurement. (This was the reason we became involved in such measurements.) A microphone at

the surface measures acoustic pressure which due to the boundary condition is also the pressure below the surface and the geophone measures displacement velocity hence we have p and u . The ratio $\frac{|p|}{|u|}$ has been measured for several soils and has been found to lie in the range $10^3 - 10^5 \rho_0 c_0$. This value is not consistent with the measurements of impedance using the reflection technique described earlier which gave $|Z|$ values from 1 to 100 times $\rho_0 c_0$. Clearly the impedance measured directly with the geophone is not the same as that measured using the reflection technique.

There are two possible sources for the large differences in impedances determined from these two techniques. The first possible explanation is that the local reaction assumption upon which all our data analysis is based is not valid. The second is that the two experiments actually measure different phenomena. Only the latter of these two possibilities is explored in the following. A careful examination of the local reaction assumption will be made in the following months when long range data allows comparisons to predicted surface wave amplitudes. As an additional justification for at least temporarily retaining the local reaction assumption, it should be noted that no measurements on any porous acoustical materials have been made which clearly indicate the assumption is not valid. Although the analysis of most such measurements are based on the local reaction assumption, it would seem that if the assumption was not valid, there would be inconsistencies noted in at least a few of the measurements (for example a value of Z that depended non-uniformly on the frequency).

Retaining the locally reacting assumption, there are several physical mechanisms to explain the large difference between the directly measured impedance and that measured using the reflection technique. The basic idea

is well developed from a study of acoustic tile. One can imagine the surface as consisting of many pores held by an elastic matrix. When the acoustic wave impinges on the surface, air is forced into the pores alternately compressing the air in them. The air being forced through the pores encounters drag due to fibers in the channel and the walls of the pores so not all of the energy flows back out of the pore as the acoustic pressure oscillates. The sound velocity in the pores is slower than in free space and highly frequency dependent. The amplitude of the sound returned to the reflected wave, then, will depend on how much energy is transferred to the matrix and the phase of the reflected wave will depend on the distance the wave travels in the pore. When all the pores are not of the same depth, reflections from different depths will add with random phases giving rise to phase cancellations.

This model is consistent with both the measured surface impedances and the seismic/acoustic ratio. At high frequencies, the seismic/acoustic ratio drops dramatically suggesting that either the energy is all being reflected back into the space above the surface or the sound energy is being converted to heat by the drag at the pore walls and oscillations of fibers in the channel. The surface impedance (real part) approaches unity at high frequencies, indicating that the wave is not being reflected hence it must be absorbed. At low frequencies, the seismic/acoustic ratio increases rapidly indicating that less energy is being absorbed in the fibrous structure, i.e., the ground plane is behaving like a simple boundary. The measured surface impedance also increases at lower frequencies indicating that Z is approaching ρc of the soil (which for our cases is of the order of 10^3). If we take 200 Hz as the crossover frequency for the two types of behavior, this suggests that the pores have a depth such that near 200 Hz, the average depth is of the order

of a half wavelength in the porous medium ($\sim 0.5 \text{ m}$ assuming $n = 1.5$). The gross frequency dependent features of Z and μ , then agree for a surface similar to acoustic tile.

There is one complicating feature which can not be ignored; the magnitude of μ . Near 100 Hz, μ has a value near $5 \times 10^{-5} \text{ cm/sec/}\mu\text{bar}$ while, for a plane interface with the measured values of ρ and c , one would predict a coupling coefficient of $1.5 \times 10^{-5} \text{ cm/sec/}\mu\text{bar}$ (Ref. 11). Considering the relative crudeness of the measurements of μ , a factor of three error does not seem unreasonable. However, the most likely direction for the error would be in the direction of less energy coupled into the ground. For now, we will assume that this factor of three does not affect our conclusions involving the physical mechanisms which give rise to the measured surface impedance. This conclusion, along with the assumption of a normally reacting surface deserves additional attention in the future.

Assuming the surface is a locally reacting porous medium, there are several approaches which can be used to characterize the surface in terms of its acoustic properties (other than impedance) which are more readily measured than impedance. The two which will be considered in detail here are those advanced by Chessell¹³ (which is an extension of the earlier work of Delaney and Bazely¹⁴) and Donato¹⁵ (which is an application of the general development by Morse¹⁶).

Chessell's approach is strictly empirical and involves only one parameter; the specific flow resistance σ (in units of $\text{gm cm}^{-3} \text{ sec}^{-1}$). The empirical relations for the acoustic impedance are

$$Xr/\rho_0 c_0 = 1 + 9.08 (f/\sigma)^{-0.75} \quad (2)$$

and
$$Xc/\rho_0 c_0 = -11.9 (f/\sigma)^{-0.73} \quad (3)$$

The expressions for the propagation coefficient $k = \alpha + i\beta$ are

$$\alpha / (\omega/c_0) = 1 + 10.8 (f/\sigma)^{-0.70} \quad (4)$$

and

$$\beta / (\omega/c_0) = 10.3 (f/\sigma)^{-0.59} \quad (5)$$

Typical results using the single parameter model are shown in Figures 9-15.

As can be seen, in each case, a value of σ can be found which gives Z values within experimental scatter of the measured values. A summary of the single parameter results is given in Table II. Although the variation in σ is not insignificant, the results are in general accord with physical intuition.

The measurements taken over a bare field in one case quite hard (WES I) and in the other water soaked (Run 15) give a much higher value for the flow resistance than do those taken from data over a grass covered surface. The value of σ for institutional grass has an intermediate value. These findings are consistent both in direction and magnitude with the direct measurements of flow resistance by Dickinson and Poak¹⁶.

Although the single parameter model appears to work well, it is not without problems. First, if values of σ are computed from measurements of X_r and X_c at individual frequencies, the value of σ is invariably found to increase with increasing frequency (See Table III). Also, in most cases, the value of σ computed from low frequency X_r values is higher than computed from low frequency X_c values. These two observations tend to suggest that the empirical relations (Eq. (2) and (3)) do not reflect the proper frequency dependence for the results reported here and that the ratio of X_r to X_c reflected in these equations is not constant but depends on the nature of the surface. Even with these problems, however, the simplicity of this approach and the relatively good agreement with experiment makes the method worthy of consideration.

Table II
Summary of Single Parameter Results
Following Chessell

Surface	σ (gm-cm ⁻³ -sec ⁻¹)	Grass height	% water
WES I	300		
WES II	130		
Run 2	100	none	
Run 3	50	none	
Run 4	100 \pm 50	0-2"	
Run 5	50	0-2"	
Run 6	150	10"	
Run 7	75	20"	
Run 8a & 8b	80	22"	10.3 %
Run 9	100	25"	8.6 %
Run 10	-	1.1 m	11 %
Runs 11 & 12	200	.5"	-
Run 15	350	0	22 %

Table III
Calculated Values of Flow Resistance
for WES I Data

f	$R/\rho_0 c_0$	σ_R	$X/\rho_0 c_0$	σ_X	σ_{avg}
100	16	195	-24	261	228
200	12	258	-17	326	292
400	6	181	-3	606	394
800	6	<u>362</u>	-11	<u>718</u>	<u>540</u>
				σ_{avg}	364

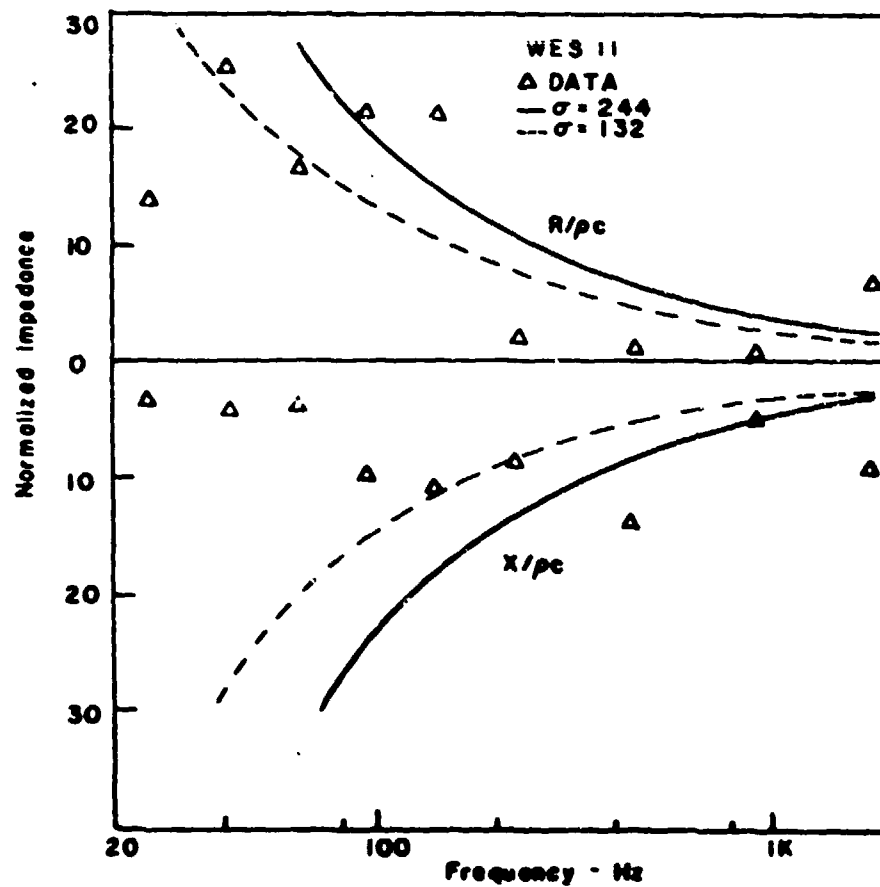
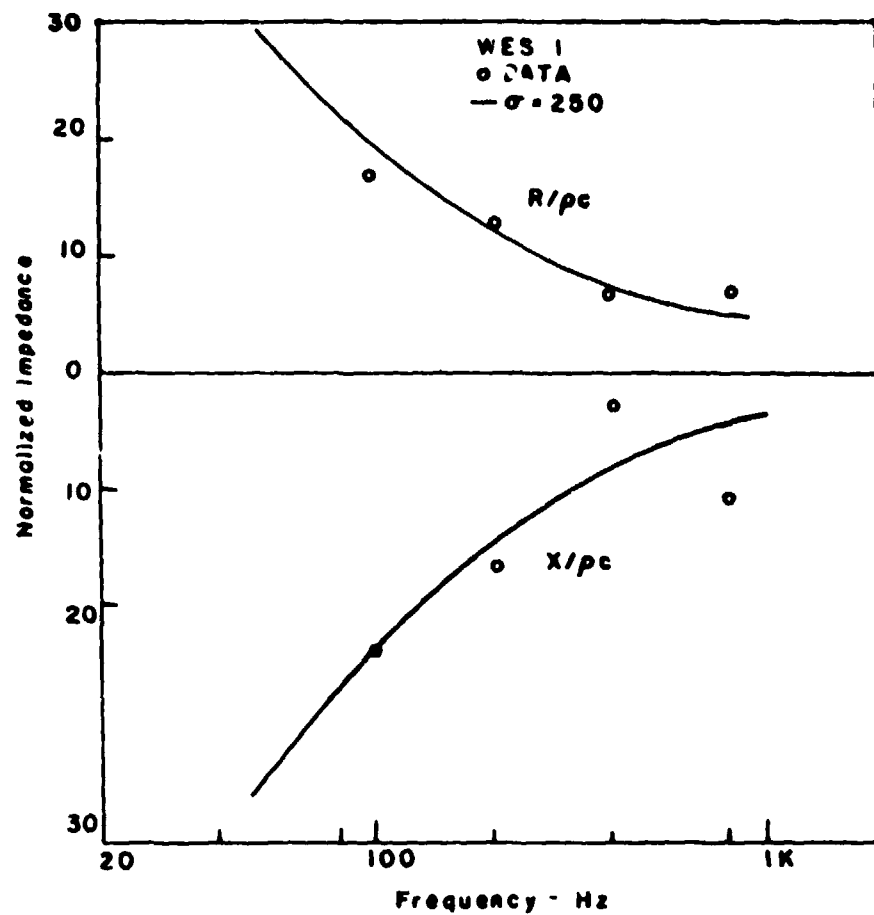


Figure 9
 34

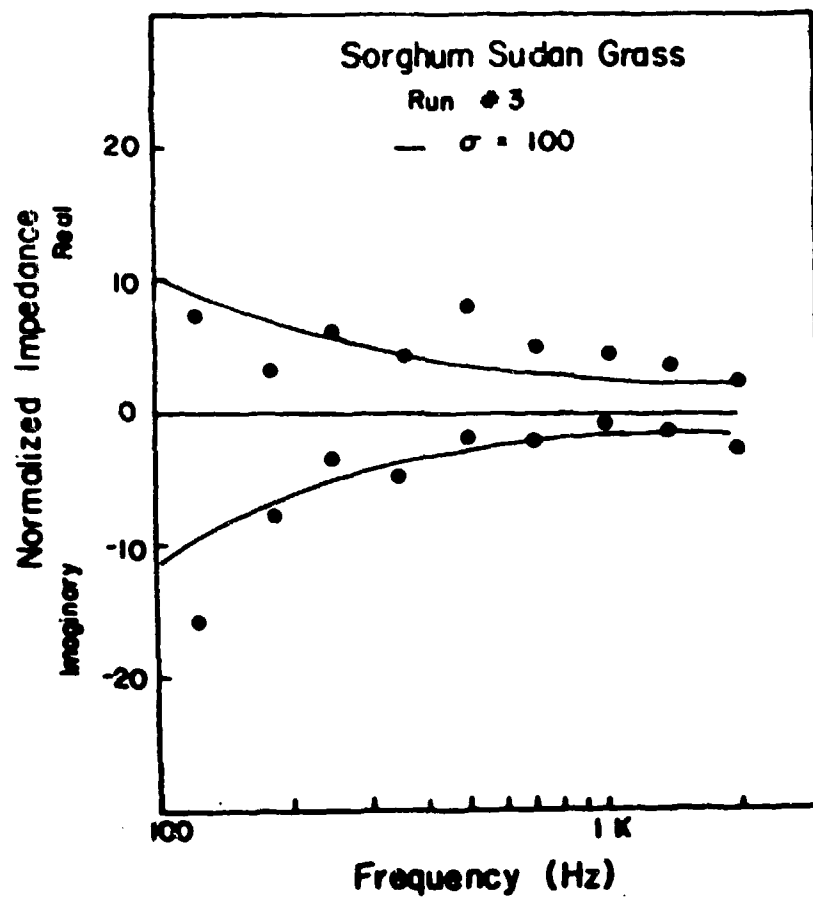
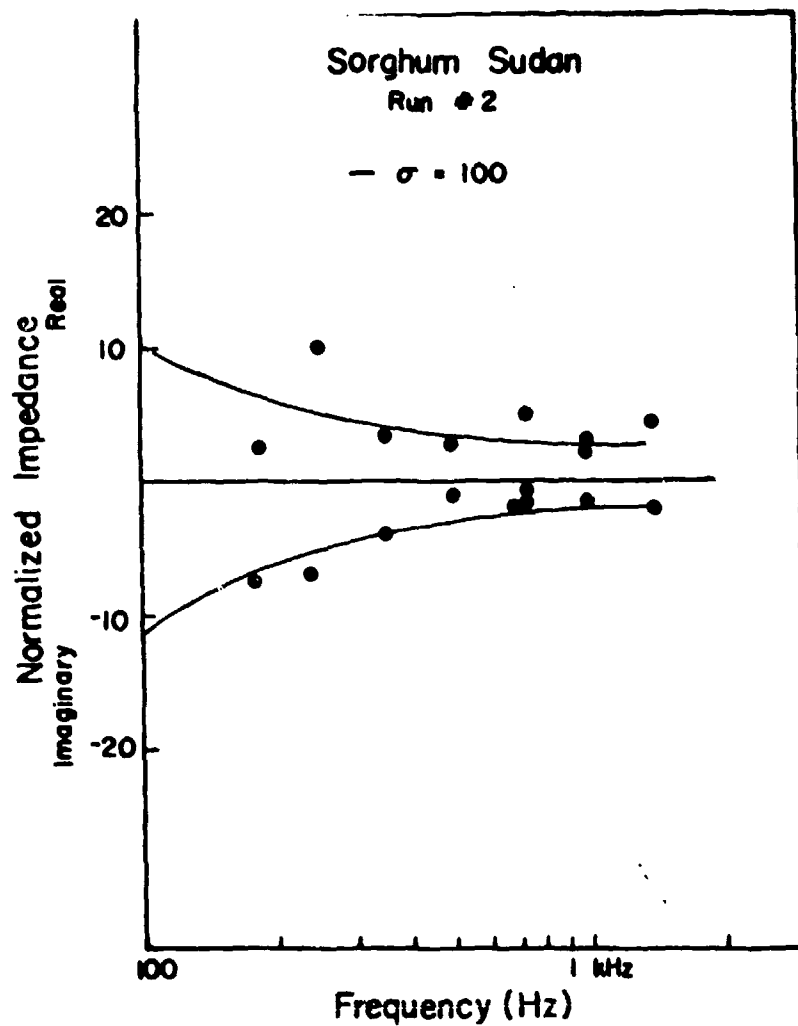


Figure 10 35

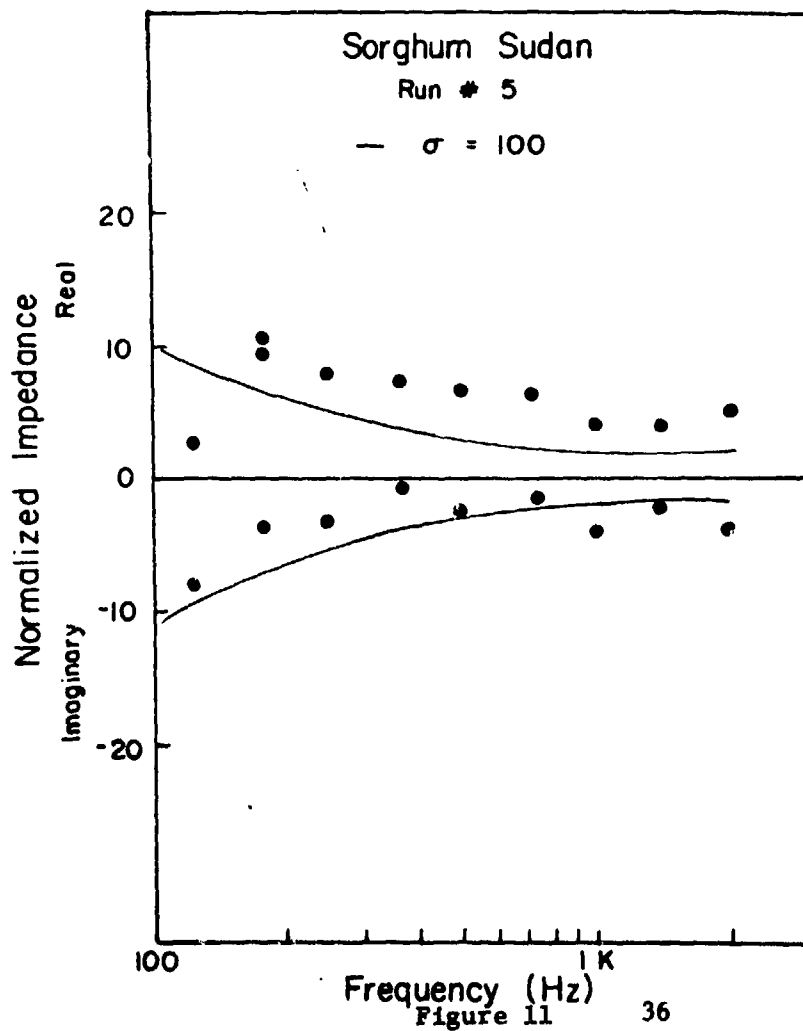
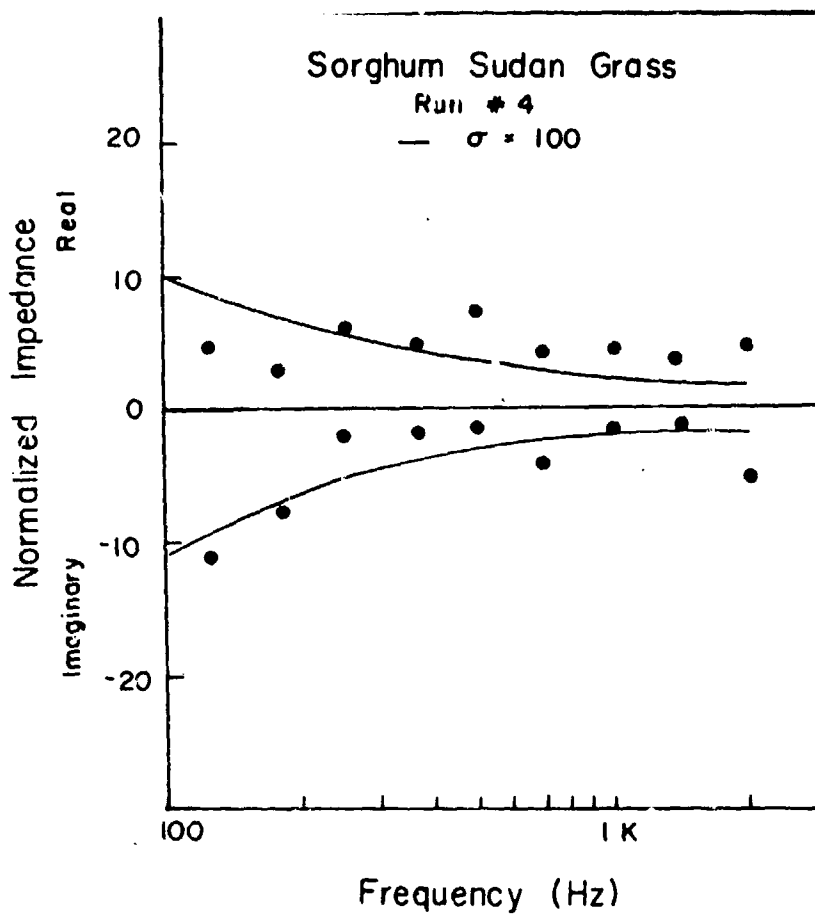
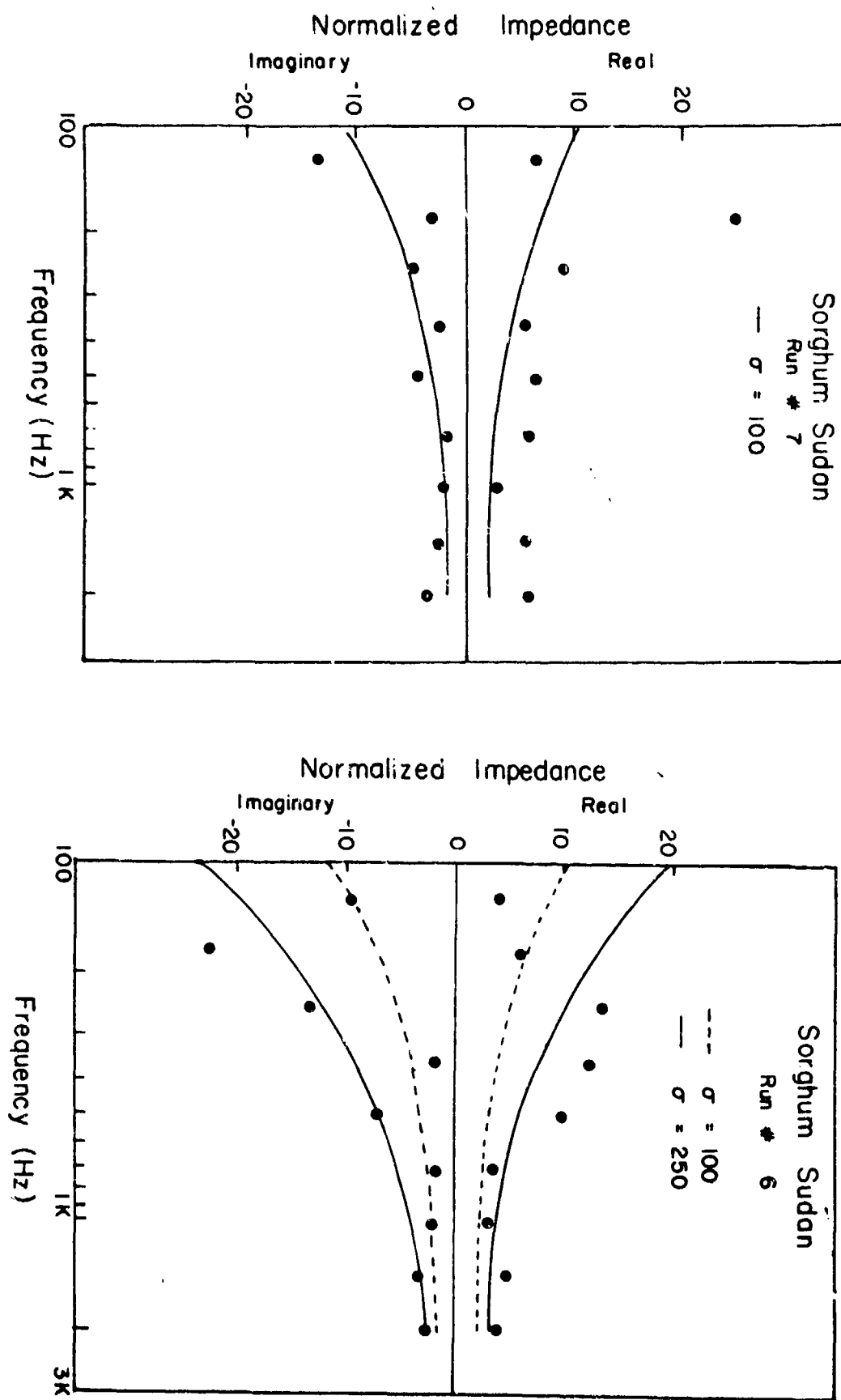


Figure 12



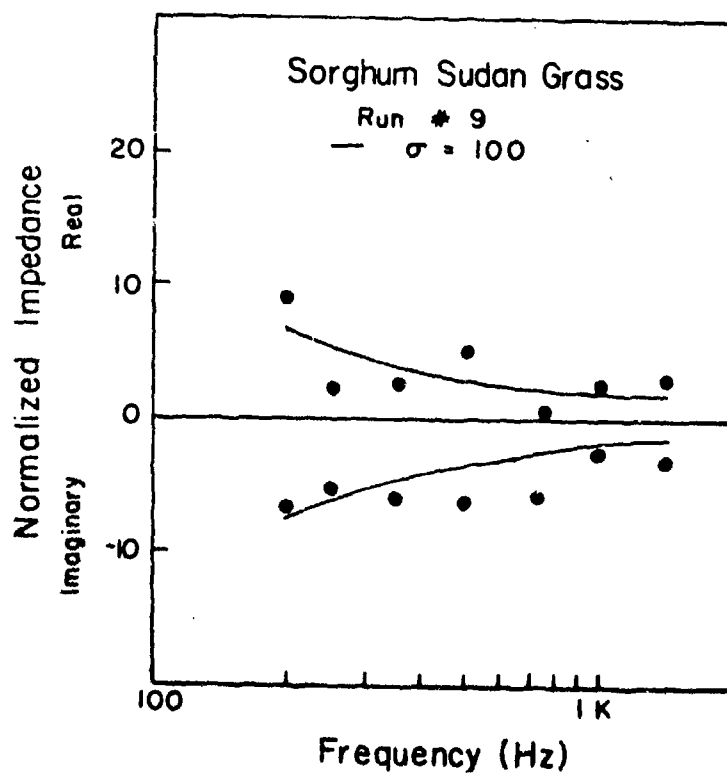
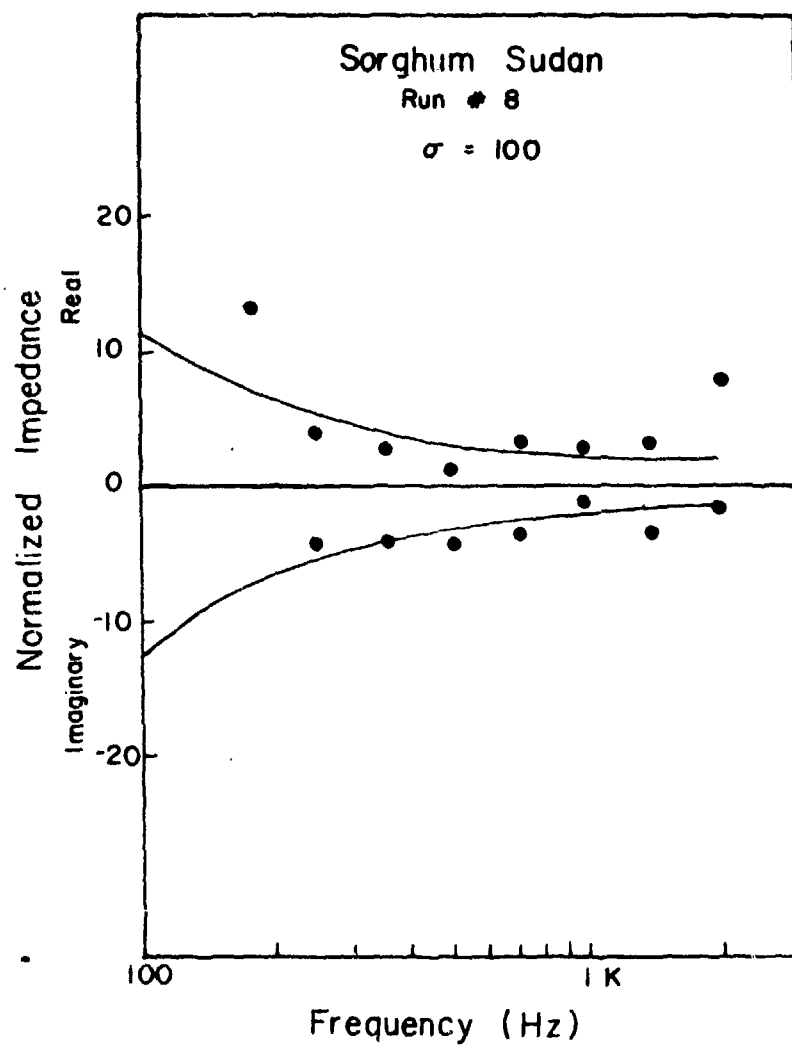


Figure 13

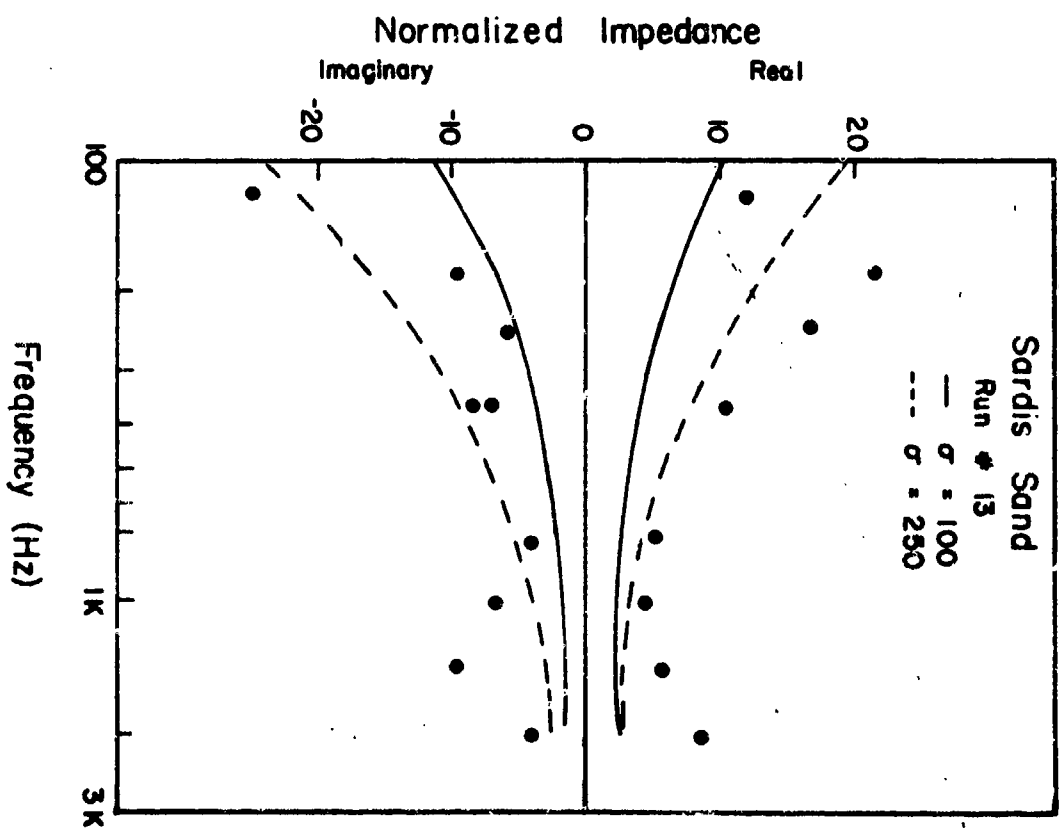
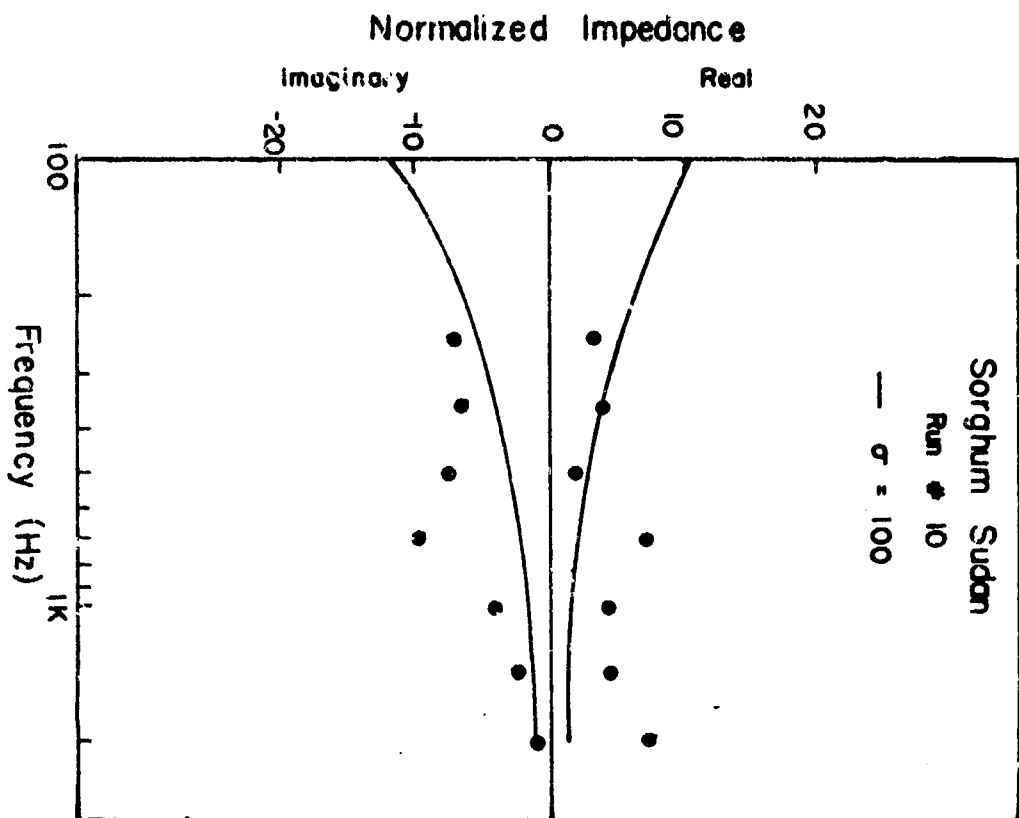


Figure 14

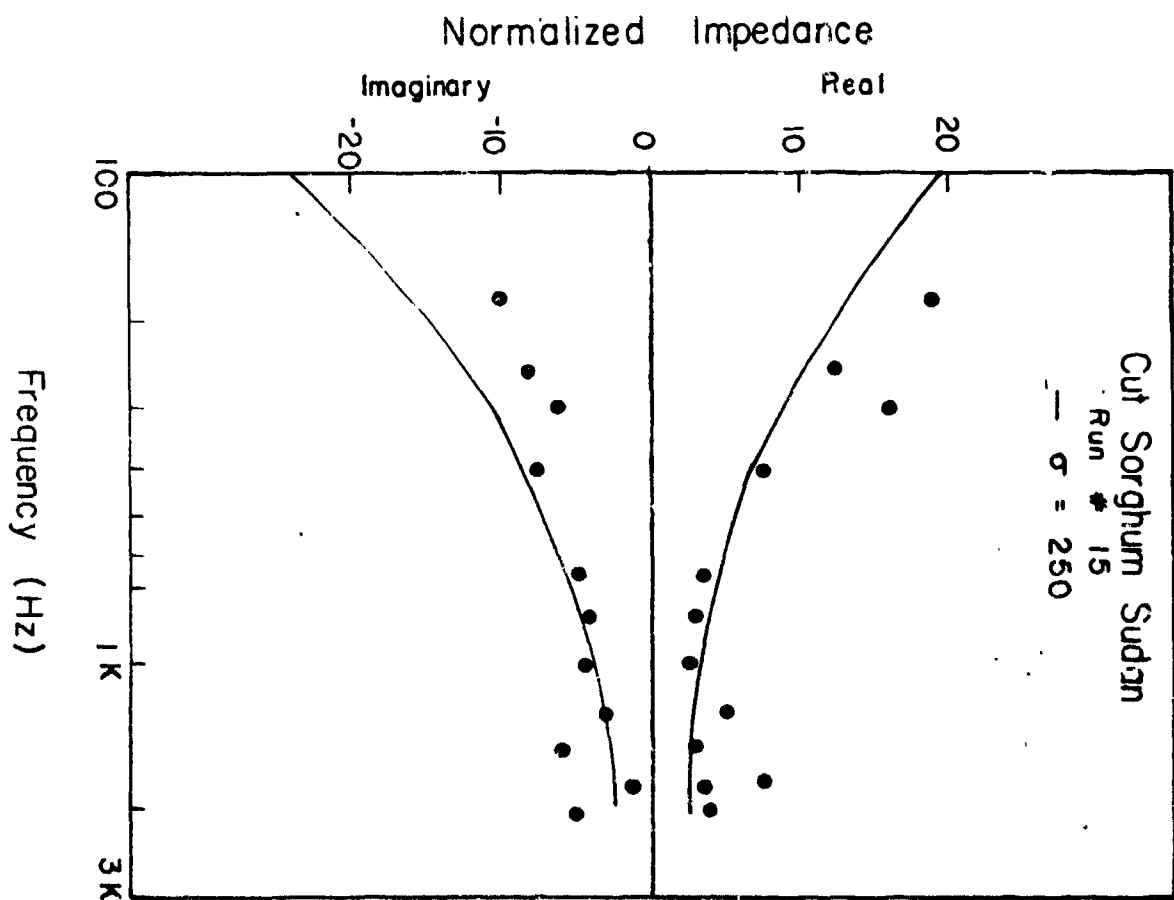
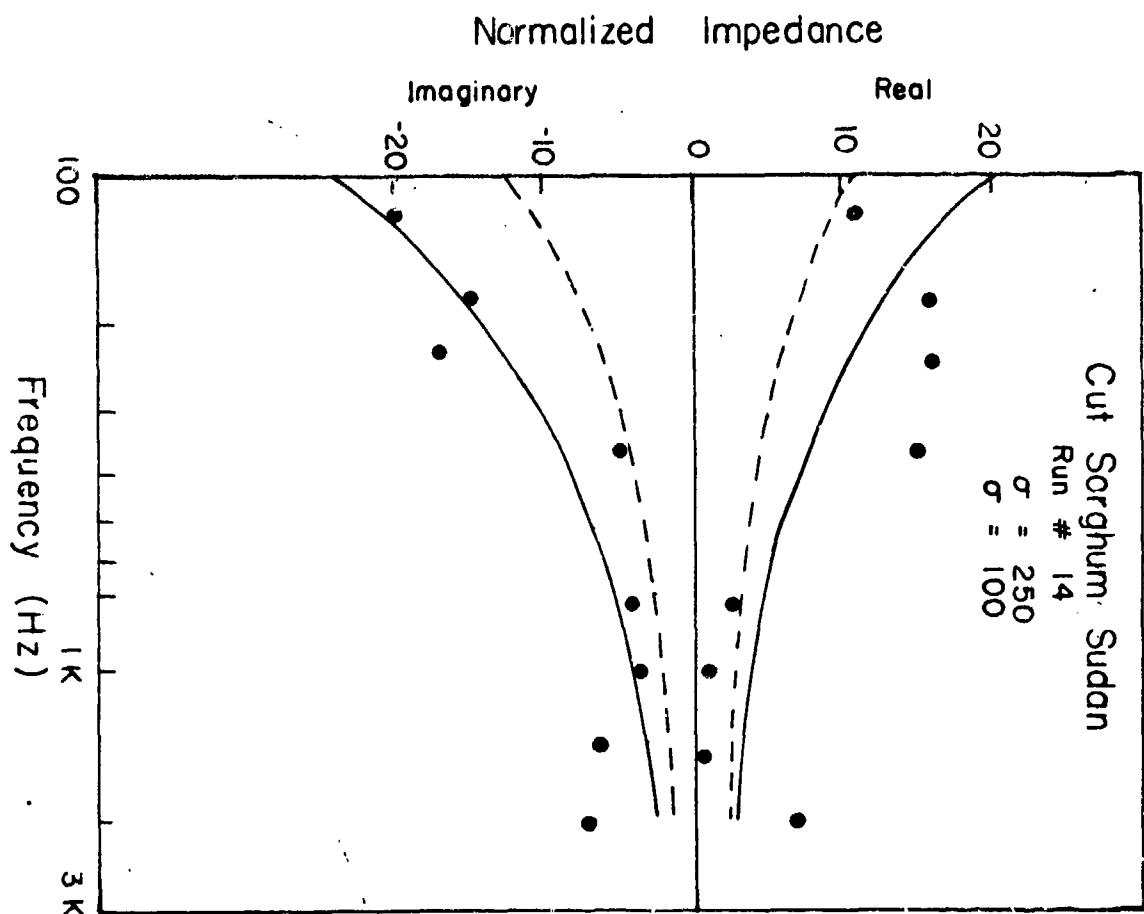


Figure 15

for field use. By measuring σ under a wide variety of conditions, tabulated values could be developed from which Z could be computed for most field conditions encountered.

Even though the empirical approach of Chessell works reasonably well for the conditions considered here, applications to other conditions would be much more reliable if the prediction procedure was based on basic physical principles. Donato¹⁴ has made an attempt to provide such a physical approach by considering three examples; a continuous porous surface, a porous medium of fixed thickness with an infinite backing, and a porous medium with a porosity which decreases exponentially with depth. Application of these three models requires that the effective compressibility of the air in the pores, K_p , the porosity, Ω , the flow resistance of the air in the pores, Φ , and the effective density of the pore-filled air ρ_p be known. Each of these terms can, at least in principle, be computed from the physical properties of the surface or measured independently, however, the formalism for such calculations has not been developed. In addition, there is a fourth case of interest; that of a porous medium backed by a medium of finite impedance. So long as each of the quantities required to apply these models must be deduced from measurements of surface impedance, this approach also becomes empirical, the only difference being that now there are more adjustable parameters available to fit the data hence, one would suppose, better agreement with theory can be achieved.

At this time, then, the single parameter empirical approach of Chessell appears to provide as good a way of representing the results as any available. From Table II, it appears that Runs 2-9 have a similar flow impedance. This suggests that the grass height has no effect on the surface impedance once the

grass has begun to grow. It also suggests that the impedance values for these runs can be averaged together to give a representation of the acoustic impedance with less scatter in the data. This is done in Figure 16 which can be considered to be the major result of the work reported here. The fact that grass height has little effect on surface impedance does not imply that the nature of the ground cover is not important. This can be seen by comparing Figure 4 for institutional grass with Figure 8 for Sorghum Sudan and Figure 15 for a bare field (with high moisture content). The bare field has a higher flow resistance than the institutional grass and both have a greater flow resistance than the Sorghum Sudan field. This result can be interpreted in terms of the root structure. The bare ground has no roots hence it has a high flow resistance. Institutional grass has a very shallow root structure and is backed by a surface which has been undisturbed for several growing seasons hence has a flow resistance less than bare ground (with no root structure) but greater than the Sorghum Sudan which has deeper roots into soil which has been recently ploughed. The bare field with all available pores filled with water represents the greatest flow resistance.

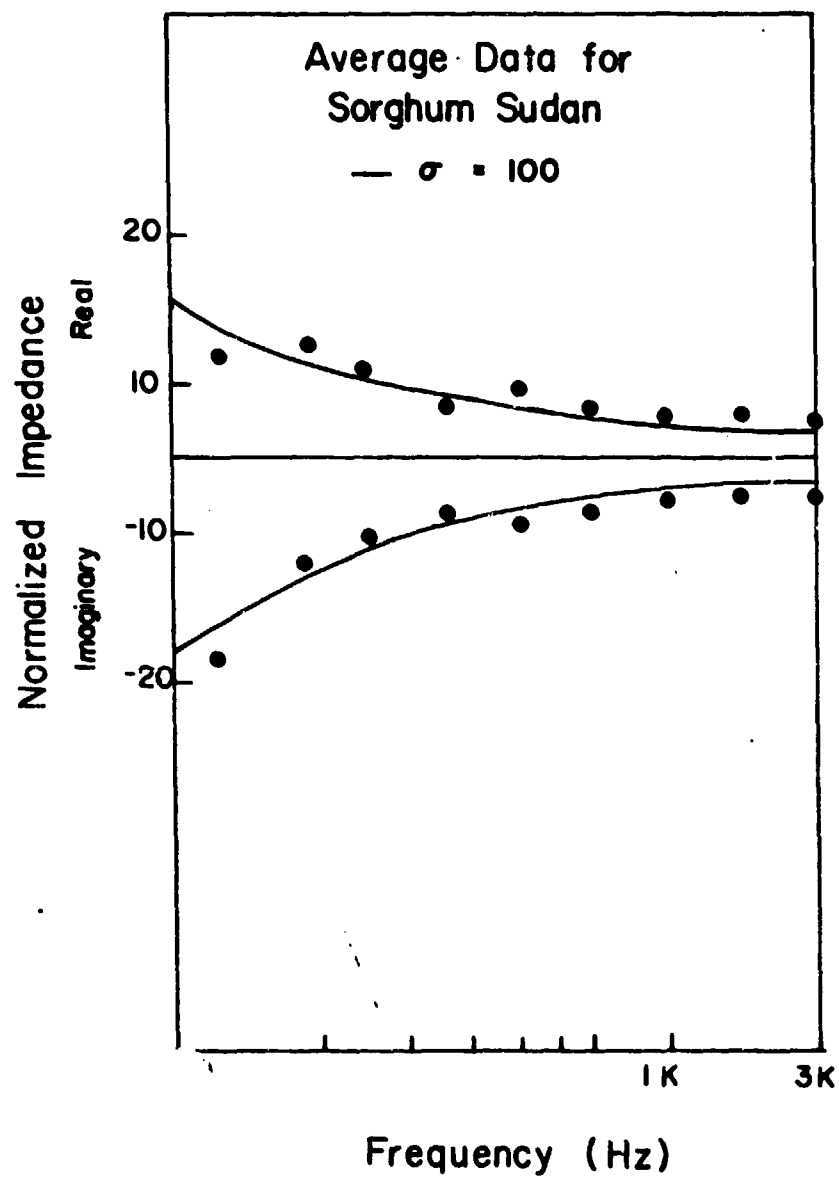


Figure 16

5.0 SUMMARY AND CONCLUSIONS

Theoretical calculations of sound amplitude near a surface with a complex impedance using the formalism developed by Donato which assumes a locally reacting surface give excellent agreement with measurements provided the complex acoustic impedance is treated as an adjustable parameter at each frequency. The significant difference between this theory and plane wave reflection theory, the existence of a surface wave, was not involved in these measurements due to the relative short ranges involved. For the measurements reported here, and earlier measurements by other investigators, the acoustic impedance as a function of frequency can be predicted within experimental uncertainty using the empirical approach of Chessell using the specific flow resistance as the single adjustable parameters. This approach has not been tested at frequencies below 100 Hz. Interpretation of the results in terms of the physical properties of the surface must await independent measurements of porosity, flow resistance, etc. or theoretical work which provide these quantities in terms of root structure and soil characteristics.

Based on the findings of this study, the following recommendations are in order:

1. Measurements of amplitude versus distance out to 1000 ft should be made in order to test theoretical predictions when the theory predicts the presence of a significant surface wave.
2. Measurements should be extended to lower frequencies to test the empirical method of computing the impedance at various frequencies using a single parameter; the specific flow resistance.

3. Independent measurements of surface and soil conditions including flow resistance should be made whenever measuring impedance in order to provide the basic data necessary to predict the impedance of a surface without making extensive measurements.

4. Measurements of surface impedance for a wide variety of surfaces are needed to supply data on which to base theoretical models applicable to the range of conditions which might be found in the field. Although all four of these recommendations will be pursued in this laboratory in the near future, item 3 requires the cooperation of others making similar measurements under different conditions.

6.0 BIBLIOGRAPHY

1. R. J. Donato, "Propagation of a Spherical Wave Near a Plane Boundary with Complex Impedance", J. Acoust. Soc. Am. 60, 34-39 (1976).
2. F. Douglas Shields and H. E. Bass, "Atmospheric Absorption of High Frequency Noise and Application to Fractional-Octave Bands", NASA CR-2760 (1977).
3. L. E. Evans, H. E. Bass, and L. C. Sutherland, "Atmospheric Absorption of Sound: Theoretical Predictions", J. Acoust. Soc. Am. 51, 1565-1575 (1972).
4. J. E. Piercy, "Role of the Vibrational Relaxation of Nitrogen in the Absorption of Sound in Air", J. Acoust. Soc. Am. 46, 602-604 (1969).
5. L. C. Sutherland, J. E. Piercy, H. E. Bass, and L. B. Evans, "Method for Calculating the Absorption of Sound by the Atmosphere", J. Acoust. Soc. Am. 56, S1(A) (1974).
6. "Proposed American National Standards Method for the Calculation of the Absorption of Sound by the Atmosphere", proposed Standard S1.26/ASA 23-197X.
7. S. P. Pao and L. B. Evans, "Sound Attenuation Over Simulated Ground Cover", J. Acoust. Soc. Am. 49, 1069-1075 (1971).
8. J. E. Piercy, T. F. W. Embleton, and L. C. Sutherland, "A Review of Noise Propagation in the Atmosphere", J. Acoust. Soc. Am. 61, 1403-1418 (1977).
9. T. W. F. Embleton, J. E. Piercy, and N. Olson, "Outdoor Propagation over Ground of Finite Impedance", J. Acoust. Soc. Am. 59, 267-277 (1976).
10. J. E. Piercy and T. F. W. Embleton, "Effect of Ground on Near-Horizontal Sound Propagation", Trans. Soc. Auto Eng., Sect. I, 83, 928-932 (1974).
11. C. B. Officer, Introduction to the Theory of Sound Transmission (McGraw-Hill, New York, 1958) Ch. 5.
12. Daniel Crass, Jerry Lundien, Henry E. Bass, and L. N. Bolen, "Acoustic-To-Seismic Coupling Properties and Applications to Seismic Sensors", Waterways Experiment Station Technical Report M-XXXX (1978).
13. C. I. Chessell, "Propagation of Noise Along a Finite Impedance Boundary", J. Acoust. Soc. Am. 62, 825 (1977).

14. M. E. Delany and E. N. Bazley, "Acoustical Properties of Fibrous Absorbent Materials", Applied Acoustics 3, 105-116 (1970).
15. R. J. Donato, "Impedance Models for Grass-Covered Ground", J. Acoust. Soc. Am. 61, 1449-1452 (1977).
16. P. M. Morse and K. U. Ingard, Theoretical Acoustics (McGraw-Hill, New York, 1968) p. 252.

Appendix

Computer Programs Used to Analyze Data

Two programs were used to analyze the data. Actually these were two variations of the same program called DONA40. The only difference between the programs is that the second accepts data for two microphone heights simultaneously. It should be noted that the input source height (IS) is in feet while the input receiver height (ZR) is in meters. Ranges are all in feet; the experimental data are in dB reference any standard position.

Both versions of the program use subroutine DONATO which is the program developed by Donato to evaluate the signal level when the impedance is known. In order to scale sound levels, subroutine SUNUP in both programs adjusts the levels such that the average is the same experimentally and theoretically (from DONATO). The subroutines PEG actually vary the impedance about some initial guess until the best fit of theory to experiment is achieved. These values are then printed out along with measured and computed sound levels.

THIS PAGE IS BEST QUALITY PRACTICABLE
FROM COPY FURNISHED TO DDG

C DUNA41 IS A EDIT OF DUNA40, CONNECTED TO OBTAIN FIRST A BALL
C PARK APPROXIMATION FOR XP AND XC AND THEN TO REFINE THESE
C TO OBTAIN ACCURACY WITHIN 0.01 OF THE RIGHT ANSWER
C WITHOUT USING SO MUCH TIME.
C XERR INPUT IS IGNORED BY DUNA40 AT PRESENT (3/16/78).

C DUNA41 IS THE FORMER RANG4N AND REPRESENTS ONLY A CHANGE IN FILE
C AND SINGLING NAME "IONATO", INSTEAD OF "COMPUT".

C RANG4N IS AN EDIT OF RANG4K, EXCLUSIVE OF INTERVIEWING EDITS.
C RANG4P WAS GUILTY OF A KIND OF SYSTEM ERROR IN SUBROUTINE PFG;
C IN THE CODE BETWEEN STATEMENTS 10 AND 50 OF SAME, XCDL AND
C XDEL WERE OCCASIONALLY HALVED. UNFORTUNATELY, NEW REMAINED
C THE SAME (OVERLOOKING THE POSSIBILITY THAT THE RIGHT VALUE
C COULD BE HALF IN THAT DIRECTION HALF THE OLD XDEL).

C ALSO, RANG4N IS THE FIRST EDIT TO ANNOUNCE ITS WORK --
C SEE WHITE(3,4).

C RANG4K IS A POLISHED VERSION OF RANG4J.
C THERE IS NO PROCEDURAL DIFFERENCE BETWEEN THE TWO.

C RANG4J IS THE EDIT OF RANG4G PATTERNED AFTER THE LATTER AND
C RANG4P IN USING EXPON CRITERIA (XERR) ON JUST THE XDEL'S AND IN
C LIMITING THE VALUES OF XDEL TO NO LOWER THAN XERR.

C THIS RANGE VERSION IS A MODIFICATION OF RANGE2, NOT RANGE3,
C THE SYSTEM OF WHICH APPEARS TO RELY ON A FALSE ASSUMPTION,
C THAT THERE IS ONLY ONE MINIMUM OF SUMSQ(XP, XC). THE
C APPARENT ERROR MAY OR MAY NOT EXIST.

C RANGE ACCEPTS THE EXPERIMENTAL DATA VALUES AND ASSESSES THE APPRO-
C PRIATE IMPEDANCE VALUES GIVING THE BEST FIT.
C THIS ROUTINE WAS DEVELOPED AND WRITTEN BY WALKER FOR H. E. HARR
C L. M. BOLEN FOR ANALYSIS OF ACOUSTIC IMPEDANCE DATA.

DIMENSION TAMI(10)
EQUIVALENCE (EXP SUM, EXP AVG), (STANDARD, SUM I)
COMMON /MAT1/ EXPDAT(10), EXP AVG, COUNT/BLK/RANGE(10), ZF, ZS/NUM/NUM
A /EPR/XERR/OLD/SUM LD

C INPUT

READ(2,1) ZS,ZR,DIL,XERR
READ(2,8) NTOTAL,NUMMAX
READ(2,1) (RANGE(I),I=1,NUMMAX)

C CRUNCH THE DATA

DO 70 N=1,NTOTAL
READ(2,9) FR,NGCN,NUM
IF(NGCN.GT.NUMMAX) NUM=NUMMAX
IF(NGCN.EQ.0) READ(2,1) XP,XC
READ(2,1) (EXP DAT(I),I=1,NUM)

EXP SUM=0.
DO 20 I=1,NUM
20 EXP SUM=EXP SUM+EXP DAT(I)
EXP AVG=EXP SUM/FLUAT(NUM)

IF(NGCN.EQ.0) CALL IMPED(FR,XP,XC)

```

XRINIT=XR;XCINIT=XC

CALL DONATO(FR,XRINIT,XCINIT,TAMP)
SUMINI=SUMUP(TAMP)
SUMOLD=SUMINI

30  NCOUNT=0
    XERR=0.1
40  CALL IEG(FR,XR,XC,DEL)
    XERR=0.01
    CALL IEG(FR,XR,XC,DEL)

50  XRDIF=(XP-XRINIT)/XRINIT*100.;XCDIFF=(XC-XCINIT)/XCINIT*100.
    CALL DONATO(FR,XR,XC,TAMP)
    SUMSQ=SUMUP(TAMP)
    SUMDIF=0.0
    DO 60 I=1,NUM
60  SUMDIF=SUMDIF+ABS(TAMP(I)-EXPLAT(I))
    STANDV=SQRT((SUMSQ-SUMDIF**2/FLOAT(NUM))/FLOAT(NUM-1))

    SUMERF=(SUMINI-SUMSQ)/SUMINI*100.

    WRITE(3,6) FR,ZS,ZP
    WRITE(3,3) XRINIT,XCINIT
    WRITE(3,7) XR,XC
    WRITE(3,5)
    WRITE(3,2) (RANGE(I),EXPDAT(I),TAMP(I),I=1,NUM)
    WRITE(3,10) STANDV,SUMSQ,NCOUNT,DEL,XERR
    WRITE(3,4) XRDIF,XCDIFF,SUMERF
70  CONTINUE

C    FORMAT STATEMENTS 2 AND 5 HAVE BEEN ALTERED TO SHORTEN OUTPUT
C    TO DESIRED INFORMATION ONLY.

1    FORMAT(8F)
2    FORMAT(1X,F7.1,6X,F7.2,4X,F7.2)
3    FORMAT(/12X,'GIVEN IMPEDANCE ',F6.2,' + ',F6.2,'I')
4    FORMAT(/8X,'IMPEDANCE DIFFERENCES ',F7.2,'% & ',F7.2,'%'/8X,
A    'SUMSQ DIFFERENCE (W.R.T. SUMINI)',F7.2,'%'/20X,
A    'DONE BY DONATO')
5    FORMAT(/3X,'RANGE',6X,'EXP. DATA ',5X,'TOTAL AMP '/
A    3X,'(FT)',9X,'(DB)',11X,'(DI)')
6    FORMAT('1',21X,'FREQUENCY',F7.1,' HZ'/16X,'SOURCE HEIGHT',F7.1
A    ', FT'/16X,'RECEIVER HEIGHT',F7.2,' FT'/)
7    FORMAT(/12X,'FINAL IMPEDANCE ',F6.2,' + ',F6.2,'I')
8    FORMAT(2I)
9    FORMAT(F,2I)
10   FORMAT(/5X,'STANDV= ',F9.5/5X,'SUMSQ= ',F9.5/5X,'TRIALS= ',I9
A    /5X,' DEL= ',F9.2/5X,' XERR= ',F9.3)

END

SUBROUTINE IEG(FR,XR,XC,DEL)
DIMENSION GENDAT(10),SUM(4),CX(4,2)
COMMON /MAIN/EXPDAT(10),EXPVGC,NCOUNT,EPR/XERR/OLD/SUMOLD

CALL DONATO(FR,XR,XC,GENDAT)
SUMOLD=SUMUP(GENDAT)
XDEL=DEL;XCDEL=DEL
XRO=XR;XCO=XC;XEM=10.*XEPH;XEW=0

```

THIS PAGE IS BEST QUALITY PRACTICABLE
FROM COPY FURNISHED TO DDC

```

C      DO ALL FOUR INITIALLY
1      DO 2 I=1,4
2      SUM(I)=SUMOLD
C      PROCEED WITH THE FIGURING
10     IF(NEW.EQ.1) GOTO 20
        CX(1,1)=XR
11     CX(1,2)=XC-XCDEL
        IF(CX(1,2).GE.0.1) GOTO 13
            IF(NEW.LE.3) GOTO 20
            IF(XCDEL.LE.XERR) GOTO 20
            XCDEL=XCDEL*0.5
            NEW=0
            GOTO 11
13     CALL DONATO(FR,CX(1,1),CX(1,2),GENDAT)
        SUM(1)=SUMUP(GENDAT)
20     IF(NEW.EQ.2) GOTO 30
        CX(2,2)=XC
21     CX(2,1)=XP-XRDEL
        IF(CX(2,1).GE.0.1) GOTO 23
            IF(NEW.LE.4) GOTO 30
            IF(XRDEL.LE.XERR) GOTO 30
            XRDEL=XRDEL*0.5
            NEW=0
            GOTO 21
23     CALL DONATO(FR,CX(2,1),CX(2,2),GENDAT)
        SUM(2)=SUMUP(GENDAT)
30     IF(NEW.EQ.3) GOTO 40
        CX(3,1)=XR
        CX(3,2)=XC+XCDEL
33     CALL DONATO(FR,CX(3,1),CX(3,2),GENDAT)
        SUM(3)=SUMUP(GENDAT)
40     IF(NEW.EQ.4) GOTO 50
        CX(4,1)=XP+XRDEL
        CX(4,2)=XC
        CALL DONATO(FR,CX(4,1),CX(4,2),GENDAT)
        SUM(4)=SUMUP(GENDAT)
50     NEW=LEAST(SUMOLD,SUM)
        NCOUNT=NCOUNT+1
        IF(NEW.EQ.0) GOTO 120
            XR=XC(NEW,1)
            XC=XC(NEW,2)
            SUMOLD=SUM(NEW)
            NEW=NEW+2
            IF(NEW.GT.4) NEW=NEW-4
        GOTO 10
120    IF((XR-XRG.GT.XEM).OR.(XC-XCO.GT.XEM)) GOTO 130
        IF(XRDEL.LE.XERR.AND.XCDEL.LE.XERR) RETURN
130    XP=XR,XC=XC
        IF(XRDEL.GT.XERR) XPDEL=XRDEL*0.5
        IF(XCDEL.GT.XERR) XCDEL=XCDEL*0.5
        GOTO 1

END

FUNCTION SUMUP(GENDAT)
DIMENSION GENDAT(10)
COMMON /MAIL/EXPDAT(10),EXPAVG,NCOUNT,NF,NRM

```


THIS PAGE IS BEST QUALITY PRACTICABLE
FROM COPY FURNISHED TO DDC

```
SUMUP=0.  
GENAVG=0.  
  
10 DO 10 I=1,NUM  
   GENAVG=GENAVG+GENDAT(I)  
   GENAVG=GENAVG/FLOAT(NUM)  
  
15 DO 15 I=1,NUM  
   GENDAT(I)=GENDAT(I)-GENAVG+EXPAVG  
  
20 DO 20 I=1,NUM  
   SUMUP=SUMUP+(GENDAT(I)-EXPDAT(I))**2  
  
RETURN  
END  
  
FUNCTION LEAST(SUMOLD,SUM)  
DIMENSION SUM(4)  
  
LEAST=1  
DO 5 I=2,4  
  IF(SUM(I).GT.SUM(LEAST)) GOTO 5  
  LEAST=I  
5 CONTINUE  
  
IF(SUMOLD.LE.SUM(LEAST)) LEAST=0  
RETURN  
END
```

C DONA40 IS A EDIT OF DONA4N, CORRECTED TO OBTAIN FIRST A BALL
C PARK APPROXIMATION FOR XR AND XC AND THEN TO REFIRE THESE
C TO OBTAIN ACCURACY WITHIN 0.01 OF THE RIGHT ANSWER
C WITHOUT USING SO MUCH TIME.
C XERR INPUT IS IGNORED BY DONA40 AT PRESENT (3/16/78).

C DONA4N IS THE FORMER RANG4N AND REPRESENTS ONLY A CHANGE IN FILE
C AND SUBROUTINE NAME "DONA0", INSTEAD OF "COMPU?".

C RANG4N IS AN EDIT OF RANG4K, EXCLUSIVE OF INTERVENING EDITS.
C RANG4N WAS GUILTY OF A MINOR SYSTEM ERROR IN SUBROUTINE PEG;
C IN THE CODE BETWEEN STATEMENTS 10 AND 50 OF SAME, XCDL AND
C XRDEL WERE OCCASIONALLY HALVED. UNFORTUNATELY, NEW REMAINED
C THE SAME (OVERLOOKING THE POSSIBILITY THAT THE RIGHT VALUE
C COULD BE BACK IN THAT DIRECTION HALF OF OLD X?DEL).

C ALSO, RANG4N IS THE FIRST EDIT TO ANNOUNCE ITS WORK --
C SEE WRITE(3,4).

C RANG4N IS A POLISHED VERSION OF RANG4J.
C THERE IS NO PROCEDURAL DIFFERENCE BETWEEN THE TWO.

C RANG4J IS THE EDIT OF RANG4G PATTERNED AFTER THE LATTER AND
C RANG4N IN USING ERROR CRITERIA (XERR) ON JUST THE X?DEL'S AND IN
C LIMITING THE VALUES OF X?DEL TO NO LOWER THAN XERR.

C THIS RANGE VERSION IS A MODIFICATION OF RANGE2, NOT RANGE3,
C THE SYSTEM OF WHICH APPEARS TO RELY ON A FALSE ASSUMPTION,
C THAT THERE IS ONLY ONE MINIMUM OF SUMSQ(XR,XC). THE
C APPARENT ERROR MAY OR MAY NOT EXIST.

C RANGE ACCEPTS THE EXPERIMENTAL DATA VALUES AND ASSESSES THE APPRO-
C PRIATE IMPEDANCE VALUES GIVING THE BEST FIT.
C THIS ROUTINE WAS DEVELOPED AND WRITTEN BY WALKER FOR H. E. BASS
C L. H. BOLEN FOR ANALYSIS OF ACOUSTIC IMPEDANCE DATA.

DIMENSION TAMP(10),AME(2,10)
EQUIVALENCE (EXPSUM,EXPVG),(STANDV,SUMDI)
COMMON /MAIN/EXPDAT(2,10),Z(2),EPAVG1,EPAVG2,IT,NCOUNT/HLT/
2 RANGE(10),ZR,ZS/NN/NUM/ERR/XERR/OLD/SUMOLD

C INPUT

READ(2,1) ZS,ZZ,DEL,XERR
READ(2,8) NTOTAL,NUMMAX
READ(2,1) (RANGE(I),I=1,NUMMAX)

C CRUNCH THE DATA

DO 70 N=1,NTOTAL
READ(2,9) FI,NGEN,NUM
IF(NUM.GT.NUMMAX) NUM=NUMMAX
IF(NGEN.EQ.0) READ(2,1) XR,XC
READ(2,1) (EXPDAT(1,I),I=1,NUM),Z(1)
READ(2,1) (EXPDAT(2,I),I=1,NUM),Z(2)

EPSUM1=0.0
EPSUM2=0.0
DO 20 I=1,NUM
EPSUM1=EPSUM1+EXPDAT(1,I)
20 EPSUM2=EPSUM2+EXPDAT(2,I)

THIS PAGE IS BEST QUALITY PRACTICABLE
FROM COPY FURNISHED TO DDQ

```

FPAVG1=EPSU1/FLOAT(NUM)
EPAVG2=EPSU2/FLOAT(NUM)

IF(NGEN.NE.0) CALL IMPED(FR,XR,XC)
XRINIT=XR;XCINIT=XC

SUMINI=0.0
DO 25 II=1,2
  ZR=Z(II)
  CALL DONATO(FR,XRINIT,XCINIT,TAMP)
  DO 23 L=1,NUM
    AMP(II,L)=TAMP(L)
  23 SUMINI=SUMUP(AMP)+SUMINI
  25 SUMULI=SUMII.I

30 NCOUNT=0
  XERR=0.1
  CALL PEG(FR,XR,XC,DEL)
  XERR=0.01
  CALL PEG(FR,XR,XC,DEL)

50 XRDIFF=(XR-XRINIT)/XRINIT*100.;XCDIFF=(XC-XCINIT)/XCINIT*100.
  DO 65 II=1,2
    ZR=Z(II)
    CALL DONATO(FR,XR,XC,TAMP)
    DO 54 L=1,NUM
      AMP(II,L)=TAMP(L)
      SUMSQ=SUMUP(TAMP)
      SUMDIF=0.0
      DO 60 I=1,NUM
        SUMDIF=SUMDIF+ABS(AMP(II,1)-EXPDAT(II,I))
      60 STANDV=SQRT((SUMSQ-SUMDIF**2)/FLOAT(NUM))/FLOAT(NUM-1)

      SUMEPP=(SUMINI-SUMSQ)/SUMINI*100.

      WRITE(3,6) FR,ZR,ZR
      WRITE(3,3) XRINIT,XCINIT
      WRITE(3,7) XR,XC
      WRITE(3,5)
      WRITE(3,2) (RANGE(I),EXPDAT(II,1),AMP(II,1),I=1,NUM)
      WRITE(3,10) STANDV,SUMSQ,NCOUNT,DEL,XERR
      WRITE(3,4) XRDIFF,XCDIFF,SUMEPP
65 CONTINUE
70 CONTINUE

C   FORMAT STATEMENTS 2 AND 5 HAVE BEEN ALTERED TO SHORTEN OUTPUT
C   TO DESIRED INFORMATION ONLY.

1   FORMAT(8F)
2   FORMAT(1X,F7.1,6X,F7.2,6X,F7.2)
3   FORMAT(//2X,'GIVEN IMPEDANCE ',F6.2,' + ',F6.2,' I')
4   FORMAT(//9X,'IMPEDANCE DIFFERENCES ',F7.2,' & ',F7.2,' %/9X,
  A 'SUMSQ DIFFERENCE (V.R.T. SUMINI)',F7.2,' %//20X,
  B 'DONE BY DONATO')
5   FORMAT(//3X,'RANGE',6X,'EXP. DATA ',5X,'TOTAL AMP ' /
  A 3X,'(BT)',6X,'(DB)',11X,'(DB)')
6   FORMAT(//11,21X,'FREQUENCY',F7.1,' HZ//16X,'SOURCE HEIGHT',F7.1
  A ', FT//16X,'RECEIVER HEIGHT',F7.2,' FT//)
7   FORMAT(//12X,'FINAL IMPEDANCE ',F6.2,' + ',F6.2,' I')
8   FORMAT(2I)
9   FORMAT(1,2I)

```

```

10  FURNAT(/5X,'STANDV= ',F9.5/5X,'SUMSQR= ',F9.5/5X,'TRIALS= ',I9
    A /5X,' DEL= ',F9.2/5X,' XEPT= ',F9.3)

    END

    SUBROUTINE IEQ(FR,XR,XC,DEL)
    DIMENSION GENDAT(2,10),GENDA(10),SUM(4),CX(4,2)
    COMMON /MATR/LX, DAT(2,10),Z(2),EP,AVG1,EP,AVG2,II,NCOUNT,BLF/
2  RANGE(10),ZP,7S/BM/NUM/EP/XEPT/OLD/SUMOLD

    SUMOLD=0.0
    DO 5 II=1,2
    ZR=Z(II)
    CALL DONATO(FR,XP,XC,GENDA)
    DO 3 L=1,NUM
    3  GENDAT(II,L)=GENDA(L)
    5  SUMOLD=SUMOLD(GENDAT)+SUMOLD
    XRDEL=DEL;XCDEL=DEL
    XRO=XP;XCO=XC;XEM=10.*XEPT;XEN=0

C    DO ALL FOUR INITIALLY

1  DO 2 I=1,4
2  SUM(I)=SUMOLD

C    PROCEED WITH THE FIGURING

10  IF(NEW.EQ.1) GOTO 20
    CX(1,1)=XR
11  CX(1,2)=X(-XCDEL)
    IF(CX(1,2).GE.0.1) GOTO 13
    IF(NEW.LE.3) GOTO 20
    IF(XCDEL.LE.XEPT) GOTO 20
    XCDEL=XCDEL*0.5
    NEW=0
    GOTO 11

13  SUM(1)=0.0
    DO 14 II=1,2
    ZR=Z(II)
    CALL DONATO(FR,CX(1,1),CX(1,2),GENDA)
    DO 15 L=1,NUM
15  GENDAT(II,L)=GENDA(L)
14  SUM(1)=SUMOLD(GENDAT)+SUM(1)
20  IF(NEW.EQ.2) GOTO 30
    CX(2,2)=X
21  CX(2,1)=XR-XRDEL
    IF(CX(2,1).GE.0.1) GOTO 23
    IF(NEW.LE.4) GOTO 30
    IF(XRDEL.LE.XEPT) GOTO 30
    XRDEL=XRDEL*0.5
    NEW=0
    GOTO 21

23  SUM(2)=0.0
    DO 25 II=1,2
    ZR=Z(II)
    CALL DONATO(FR,CX(2,1),CX(2,2),GENDA)
    DO 24 L=1,NUM
24  GENDAT(II,L)=GENDA(L)
25  SUM(2)=SUMOLD(GENDAT)+SUM(2)
30  IF(NEW.EQ.3) GOTO 40
    CX(3,1)=X

```

```

33      CX(3,2)=X1+XCDEL
      SUM(3)=0.0
      DO 35 II=1,2
      ZR=Z(II)
      CALL DONATO(FR,CX(3,1),CX(3,2),GENDA)
      DO 34 L=1,NUM
34      GENDAT(II,L)=GENDA(L)
35      SUM(3)=SUMUP(GENDAT)+SUM(3)

40      IF(NEW.EQ.4) GOTO 50
      CX(4,1)=XP+XRDEL
      CX(4,2)=XC
      SUM(4)=0.0
      DO 45 II=1,2
      ZR=Z(II)
      CALL DONATO(FR,CX(4,1),CX(4,2),GENDA)
      DO 44 L=1,NUM
44      GENDAT(II,L)=GENDA(L)
45      SUM(4)=SUMUP(GENDAT)+SUM(4)
50      NEW=LEAST(SUMOLD,SUM)
      NCOUNT=NCOUNT+1
      IF(NEW.EQ.0) GOTO 120
      XP=CX(NEW,1)
      XC=CX(NEW,2)
      SUMOLD=SUM(NEW)
      NEW=NEW+2
      IF(NEW.GT.4) NEW=NEW-4
      GOTO 10

120     IF((X1-XR0.GT.XEM).OR.(XC-XC0.GT.XEM)) GOTO 130
      IF(XRDEL.LE.XERR.AND.XCDEL.LE.XERR) RETURN
130     XR0=X1;XC0=XC
      IF(XRDEL.GT.XERR) XRDEL=X1-DEL*0.5
      IF(XCDEL.GT.XERR) XCDEL=XCDEL*0.5
      GOTO 1

END

FUNCTION SUMUP(GENDAT)
  DIMENSION GENDAT(2,10)
  COMMON /MAIN/EXPDAT(2,10),Z(2),EPAVG1,EPAVG2,II,NCOUNT/BLA/
2  RANGE(10),ZF,ZS /NM/NUM
  SUMUP=0.
  GENAVG=0.

  EPAVG=EPAVG1
  IF(II.EQ.2)EPAVG=EPAVG2
  DO 10 I=1,NUM
10  GENAVG=GENAVG+GENDAT(II,I)
     GENAVG=GENAVG/FLOAT(NUM)

  DO 15 I=1,NUM
15  GENDAT(II,I)=GENDAT(II,I)-GENAVG+EPAVG

  DO 20 I=1,NUM
20  SUMUP=SUMUP+(GENDAT(II,I)-EXPDAT(II,I))*2

  RETURN
END

FUNCTION LEAST(SUMOLD,SUM)

```

DIMENSION SUM(4)

LEAST=1

DO 5 I=2,4

IF(SUM(I),GL,SUM(LEAST)) GOTO 5

LEAST=I

5

CONTINUE

IF(SUMOLD,LE,SUM(LEAST)) LEAST=0

RETURN

END

```

C      THIS FILE CONTAINS THE SUBROUTINE "DONATO" AND ITS AUXILIARY
C      ROUTINES AS MODIFIED FROM THE ORIGINAL "GPOKD1.F4" BY WALKER
C      FOR W. E. MASS AND L. N. POLEI.

C      "DONATO" IS THE FIRMER "COMPUT" ("COMPU3" FOR FILE NAME) AND
C      REPRESENTS NO SIGNIFICANT MODIFICATIONS.

C      "DONATO" HAS ITS OWN INTERNAL COMMON "DUMPT".

SUBROUTINE DONATO(FR,XR,XC,IAMP)
  REAL Y
  DIMENSION IAMP(10)
  COMPLEX AIMP,C,SO,W,WK,TOTINT,AMP1,AMP2,AMP3,AMP4,F,D
  EXTERNAL ATAND,ATANH
  COMMON /BLK/RANGE(10),ZF,ZS/WI/HU/TINY/W,SO,K,K2,Y
  DATA PI/3.14159265/

C      CONVENTION-HAVE IN FORM EXP(IKR-IWT) AND STIFFNESS
C      REACTANCE POSITIVE IMAGINARY

14     AIMP=CMPLX(XR,XC)

C      DETERMINATION OF POLE LOCATION FROM AIMP=COS(ANGP+IANCI)+1.=0.

      B=AIMAG(AIMP)/(AIMP*CONJG(AIMP))
      A=REAL(AIMP)/(AIMP*CONJG(AIMP))
      IF(B.E.0.) GOTO 20
10     SHINE=0.
      SINE=SQRT(1.-A**2)
      GO TO 30
20     SHINE=SQRT((B**2+A**2-1.+SQRT((B**2+A**2-1.)**2+4.*B**2))/2.)
      SINE=B/SHINE
30     IF(SINE.LT.1.0)GO TO 50
40     ANGR=90.
      COSE=0.
      GO TO 60
50     COSF=SQRT(1.-SINE**2)
      ANGH=-ATAND(SINE/COSE)+180.
60     CUSHE=SQRT(1.+SHINE**2)
      K=2.*PI*FR/1132.

      DO 160 I=1,NUM
      N=RANGE(I)

C      CHECK WHETHER SURFACE WAVE EXISTS

      ANGLE=90.-ATAND((ZS+ZK)/A)
      CSHNW=1./COSD(ANGH-ANGLE)

C      CALCULATION OF SO**2. SO IS STEEPEST DESCENTS INTEGRATION
C      VARIABLE, S, CALCULATED AT POLE LOCATION

      C=(1.,0.)*SIND(ANGR-ANGLE)*SHINE+(0.,1.)*(1.-COSD(ANGP-ANGLE))
2     *CUSHF
      SO=CSQRT(C)

C      Y SET FOR INTEGRATION IN INT2

      Y=1.
      IF(AIMAG(SO).LT.0.)Y=-1.

```

```

C      R1,R2, SLANT DISTANCES SOURCE-RECEIVER, AND SOURCE IMAGE-
C      RECEIVER

      R1=SQRT((R**2+(ZS-ZH)**2))
      R2=SQRT((R**2+(ZS+ZH)**2))

C      STEEPEST DESCENTS INTEGRATION FOR LARGE K*P2*S0**2

      W=1./CSQRT(1+P2*S0**2)
      IF(CABS(K*R2*S0**2).LE.10.) CALL INT2(AMPR,AMPI,800)
70      WW=(0.5*W*(1.+0.5*W**2*(1.+1.5*W**2)))
      AMPR=REAL(WW)
      AMPI=-AIMAG(WW)

C      AMP1+AMP2 RESULT OF STEEPEST DESCENTS

80      TOTINT=CMPLX(AMPR,AMPI)
      AMP1=TOTINT*4./((AIMP*CSQD(ANGLE)+1.)*SQRT(F/R)*S0*(1.+S0*
2      ((0.,.25)*S0+((0.5-0.5*(0.,1.))*CSQD(ANGLE)/SINH(ANGLE))))
      AMP2=1./((AIMP*CSQD(ANGLE)+1.)*(1./SQRT(R*R2))*S0*((0.,0.5)*
2      S0+((1.-0.,1.0))*CSQ(ANGLE)/SINH(ANGLE)))

C      AMP4-DIRECT + PERFECTLY REFLECTED WAVES

      AMP4=(1./R2+1./R1*CEXP((0.,-1.0)*K*(R2-R1)))

C      TAKE THIS BRANCH IS PLANE WAVE CANCELLATION

110      IF(ABS(CSHH).GT.ABS(CSHF))GO TO 130

C      SURFACE WAVE IF POLE LIES WITHIN STEEPEST DESCENTS CONTOUR

      D=CSQRT(CMPLX(SINH*CSH,COSE*SHINE))

C      CORRECTION FOR PHASE DIFF SURFACE/REFLECTED

      P=(PI/4.+K*P2*CSQ(ANGR-ANGLE)*COSHE-K*R2)
      F=CEX1(CMPLX(0.,P))
      F=EXP(-K*R2*SINH(ANGR-ANGLE)*SHINE)
      AMP3=SQRT(K*2.*PI/P)*2./AIMP*F*F/(1.-(0.,1.)*1./(8.*K*R))
2      *(0.,1.0)

C      AMP3-SURFACE WAVE

      IF(CABS(AMP3).LT.1.E-30) AMP3=0.

C      MACHINE PROTECTION AGAINST TOO SMALL AMPLITUDES. ANY SURFACE
C      WAVE AMPLITUDE <10**(-30) CALL -600 DF

      GO TO 140
130      AMP3=0.
140      AMPT=(AMP1+AMP2)*CMPLX(1.,-1.0/(8.0*K*R))+AMP3+AMP4
      TAMP(1)=AMPT*CONJG(AMPT)
      TAMP(1)=10.*ALOG10(TAMP(1))
160      CONTINUE
      RETURN
      END

C      INTEGRATION PROCEDURE

      SUBROUTINE INT2(AMPR,AMPI,*)

```


THIS PAGE IS BEST QUALITY PRACTICABLE
FROM COPY FURNISHED TO DDC

```

REAL K
COMPLEX AMPNEW,W,S0,VAL,VALUE
COMMON /TINY/W,S0,K,R2,Y
EXTERNAL VALUE
AMPNEW=(0.,0.)
DEL=.05*CABS(W)
Z=-DEL
DO 10 I=1,1000
Z=Z+DEL
IF(Z.GE.2.5)GO TO 20
VAL=CMPLX(0.,0.)
VAL=VAL+VALUE(Z)/3.
VAL=VAL+VALUE(Z+DEL/2.)/3.*4.
VAL=VAL+VALUE(Z+DEL)/3.
10 AMPNEW=AMPNEW+VAL
20 AMPNEW=(0.,1.)*AMPNEW*DEL/2.*Y
AMPR=REAL(AMPNEW)
AMPI=ATNAG(AMPNEW)
RETURN 1
END

```

```

COMPLEX FUNCTION VALUE(Z)
REAL K
COMMON /TINY/W,S0,K,R2,Y
COMPLEX S0,W
VALUE=CEXP(-(Z**2)+2.*(0.,1.)*CSQRT(K*R2*(S0**2))*Z*Y)
RETURN
END

```

```

FUNCTION ATAND(X)
ATAND=ATAN(X)*180./3.14159265
IF(ATAND.GT.180.)ATAND=-180.
RETURN
END

```

```

FUNCTION ATANH(X)
DATA F1/3.14159265/
IF(X**2.GE.1.)GO TO 10
ATANH=(0.5*ALOG10((1.+X)/(1.-X)))*180./F1
RETURN
10 ATANH=(X+X**3/3.+X**5/5.+X**7/7.+X**9/9.+X**11/11.)*180./F1
20 RETURN
END

```

```

SUBROUTINE IMPEL(FR,XR,XC)
IF(FR.GT.300.)GO TO 10
XR=47.-15.*ALOG10(FR)
XC=74.-25.*ALOG10(FR)
RETURN
10 IF(FR.GT.600.)GO TO 20
XR=40.-12.*ALOG10(FR)
XC=62.-20.*ALOG10(FR)
RETURN
20 IF(FR.GT.1000.)GO TO 30
XR=28.-8.*ALOG10(FR)
XC=37.-11.*ALOG10(FR)
RETURN
30 IF(FR.GT.1500.)GO TO 40
XR=27.-8.*ALOG10(FR)
XC=25.-7.*ALOG10(FR)
RETURN

```

THIS PAGE IS BEST QUALITY PRACTICAL
FROM COPY FURNISHED TO DDC

```
40  I(FR.CT.3000.)IN T1 50  
    XH=9.-2.*ALOG10(FR)  
    XC=13.-3.*ALOG10(FR)  
50  RETURN  
    XH=2.0  
    XC=2.0  
    RETURN  
    END
```